VACANCIES AND HYDROGEN IN SIMPLE METALS

AN EXPERIMENTAL AND THEORETICAL INVESTIGATION OF VACANCIES AND HYDROGEN IN SIMPLE METALS

By

ZORAN D. POPOVIĆ, M.Sc.

A Thesis

Submitted to the School of Graduate Studies

in Partial Fulfilment of the Requirements

for the Degree

Doctor of Philosophy

McMaster University

July 1974

DOCTOR OF PHILOSOPHY (1974)
(Materials Science)

McMASTER UNIVERSITY
Hamilton, Ontario

TITLE : An Experimental and Theoretical Investigation of Vacancies and Hydrogen in Simple Metals

AUTHOR: Zoran D. Popović, M.Sc.

SUPERVISORS: Drs. G. R. Piercy and J. P. Carbotte

NUMBER OF PAGES: (vi), 148

ABSTRACT

An improved theory of vacancy formation energy and volume, based on local pseudopotential theory, is presented and applied to vacancies in the alkali metals and in aluminum. Good agreement with the existing experimental results is obtained.

The solubility of hydrogen in magnesium has been measured in the temperature interval 400°C - 600°C and for pressures 50 - 760 mmHg, from which the heat of solution of hydrogen has been determined.

A theory of the heat of solution of hydrogen is developed. The host lattice is treated with the local pseudopotential theory:

Nonlinear theory is used for the screening of the proton and a method for an approximate self-consistent solution proposed. The theoretical results for the heats of solution in aluminum and magnesium are in good agreement with the experimental values, particularly when one considers the magnitude of the numbers involved.

To My

Parents

Damjan

and

Delija

Popović

ACKNOWLEDGEMENTS

I wish to express my appreciation to Dr. G. R. Piercy and Dr. J. P. Carbotte for their guidance and encouragement throughout the course of this work. I am also grateful to Dr. M. Stott from Queen's University for his help in treating nonlinear screening of a proton, and to M. Leger and F. Kus for many helpful discussions.

At the point of acquiring the highest academic degree I would like to remember the people who influenced my education in the physical sciences: Dr. D. Tjapkin of the University of Belgrade who taught me the basic principles of solid state physics and my highschool teacher Mrs. S. Krstić with her imaginative lectures in elementary mathematics.

During the work on the thesis with its unavoidable ups and downs the patience, support and encouragement of my wife Jadranka Rizoniko-Popović has been of great help.

The competence and reliability of Miss Erie Long, who typed this thesis, has been very much appreciated.

The financial assistance through a McMaster Benefactors Scholarship and the International Nickel Company of Canada Graduate Research Fellowship is gratefully acknowledged.

TABLE OF CONTENTS

CHAPTER		PAGE
I	INTRODUCTION	1
	1.1 Scope of the Thesis	3
II	MEASUREMENT OF THE SOLUBILITY OF HYDROGEN IN SOLID MAGNESIUM	8
	2.1 Description of the Experimental Method	8
	2.2 Results of the Measurements	13
III	REVIEW OF LOCAL PSEUDOPOTENTIAL THEORY	23
	3.1 Basic Ideas of Pseudopotential Theory	23
	3.2 Pseudopotential Calculation of the Total Crystal Energy	26
	3.3 Perfect Crystal	30
IV	PSEUDOPOTENTIAL CALCULATION OF VACANCY FORMATION ENERGY AND VOLUME IN ALKALI METALS AND ALUMINUM	34
	4.1 Vacancies and Pseudopotentials - General Discussion	34
	4.2 Crystal with a Vacancy	37
	4.3 Calculation of Formation Energy and Volume of a Vacancy	40
	4.4 Results of Calculations and Discussion	47

TABLE OF CONTENTS - continued

CHAPTER		PAGE
V	THEORY OF THE HEAT OF SOLUTION AND SCREENING OF HYDROGEN IN ALUMINUM AND MAGNESIUM	52
	5.1 Formulation of the Problem	52
	5.2 Linear Response Theory of the Heat of Solution of Hydrogen in Simple Metals	55
	5.3 Nonlinear Theory for the Screening of a Proton in a Uniform Electron Gas	61
	5.4 Approximate Self-Consistent Solution of Nonlinear Proton Screening	70
	5.5 Nonlinear Proton Screening Corrections to the Heat of Solution of Hydrogen	81
VI	GENERAL DISCUSSION AND CONCLUSIONS	88
APPENDICES		
A	LATTICE STATICS OF CLOSE PACKED HEXAGONAL METALS: VACANCY IN MAGNESIUM	92
B	THE INFLUENCE OF LATTICE STRAIN ON THE RESIDUAL RESISTIVITY OF DILUTE ALKALI ALLOYS	111
C	ON THE DISPLACED LATTICE CHARGE AND RESIDUAL RESISTIVITY	124
D	SHORT DESCRIPTION OF COMPUTER PROGRAMS	142
REFERENCES		144

CHAPTER I

INTRODUCTION

A perfect crystal comprising a flawlessly ordered array of atoms is a fictional idealization of solid state theorists. Real crystalline materials can never be perfect; some disorder must always be present to a larger or smaller extent. The degree of perfection depends on the history of the crystalline material and with suitable experimental conditions we can make them less imperfect, but never completely perfect. That is a consequence of a universal law of nature which favours disorder at the expense of the order, most commonly known as the second law of thermodynamics. As a fictitious perfect crystal is an ideal starting point for understanding basic properties of real crystalline solids, the simplest imperfections, point defects are the natural starting point for investigating the defective crystalline solid state. The very name point defect suggests that the departure from perfection is limited to a small region of space. It is usually on the scale of one or two atomic volumes, with the lattice distortions due to the point defect, dying away quickly within a few atomic distances. There are two distinct types of point defects characterized by the position of the atom bringing disorder.

If the atom of a different kind substitutes an atom of the host lattice, we have a substitutional impurity. A special case of this type of imperfection is a vacancy, one atom missing in an otherwise perfect lattice. The second type of point defect represents one atom more, of the same or different kind as the host lattice atoms, situated in the space between the atoms of the perfect lattice. This type is called an interstitial impurity, or a selfinterstitial if the atom is of the same kind as the host lattice.

Point defects play an important role in determining the properties of metals. To be able to control their influence, it is important to gain knowledge about the interactions between defects and atoms of the host lattice, and between different types of defects. On the microscopic level the problem is complicated. The interactions between metallic ions are critically modified by the presence of the electron gas which screens the ionic potentials. For nontransition metals, in which the ion cores are small relative to the interatomic distances, the interactions between atoms are mainly due to Coulomb terms and thus controlled by the electrostatic potential due to each ion plus its screening electrons. They typically have an oscillatory nature, and qualitatively look something like Figure 5.1 (page 79).

In recent years a large amount of work has been done on point defects and their interactions. One of the most

important practical fields driving this field of research is nuclear technology. Application of nuclear power for satisfying ever growing energy needs has become a necessity. Under strong radiation conditions and high temperatures, mobile point defects are present in large numbers and can critically influence the properties of these materials. They are also influenced by gas atoms such as hydrogen or oxygen that dissolve in the material during its use.

1.1 Scope of the Thesis

We have chosen to treat two types of point defects: vacancies, and hydrogen atoms which are usually interstitial impurities. Our major interest is to investigate the electron screening of hydrogen. However, the vacancy problem is theoretically much simpler as only atoms of the matrix are involved and useful knowledge and experience could be obtained by studying vacancies first.

A vacancy can be regarded as the simplest impurity of the substitutional type. It is just a lack of one atom of the same kind as the matrix lattice. All metallic ions are still the same and the vacancy problem is essentially the problem of a different ionic configuration. In the last decade a method has been developed to treat the behaviour of

electrons screening ions in metals using self-consistent first order perturbation theory, which is known as pseudopotential theory (Harrison 1966). As we will show, it can be successfully applied to determine the formation energy and formation volume of vacancies, at least in metals with simple electronic structure. The pseudopotential theory for transition metals, which have much more complicated structure, is at present in the developing stage and has not yet achieved the degree of accuracy necessary for point defect calculations (Harrison 1970).

Although the work done in the thesis is of a very fundamental nature, hydrogen as an object of study has been chosen for practical reasons. It is well known how dramatically hydrogen can change properties of metals (Smialowski 1962, Kolachev 1968). One example is the formation of gas bubbles in the metal after solidification due to dissolved hydrogen. In aluminum the bubbles formed near the surface produce undesirable blistering. Another example is hydrogen embrittlement in steel, which has been and still is a great problem. Despite its practical significance, theoretical understanding of the behaviour of hydrogen dissolved in metals has not gone very far. We, therefore, felt that the theoretical investigation of hydrogen in simple metals (simple meaning simple electronic structure), combined with some experiments which would test

the theory could be a valuable contribution to a better understanding of the nature of hydrogen dissolved in metals.

The hydrogen ion, the proton, being a point charge is a very strong perturbation to the electron gas and one cannot expect first order perturbation theory to work satisfactorily. For treating hydrogen screening it is necessary to use a method based on the numerical solution of the Schroedinger equation. This method is usually referred to as the density functional formalism and the theoretical foundations for it were given by Hohenberg and Kohn (1964) and Kohn and Sham (1965).

The property on which we have chosen to test our screening theory for dissolved hydrogen is the heat of solution of hydrogen in aluminum and magnesium. These metals have a simple electronic structure and absorb measurable amounts of hydrogen in the solid state. For aluminum the solubility of hydrogen has been measured for a range of temperatures (Eichenauer 1968). The heat of solution has been deduced from the slope of the logarithmic plot of solubility versus reciprocal temperature. For solid magnesium the solubility has been measured only at 640°C (Koeneman and Metcalfe 1959). In order to obtain the heat of solution we have measured the solubility in the range 400 - 600°C.

Experimental measurements of the solubility of hydrogen in magnesium are given in Chapter II. In Chapter

III the summary of pseudopotential theory necessary for treating vacancies and a simple model of hydrogen is presented. Chapter IV deals with pseudopotential theory of vacancy formation energies and volumes in alkali metals and aluminum. In calculating properties of vacancies we have also included the effects of lattice relaxations around the defect. In Chapter V the theory for the heat of solution of hydrogen is developed. For vacancies in Al and Mg the atomic relaxations do not contribute significantly to the energy and, therefore, we have not included the effects of lattice relaxation on the heat of solution of hydrogen, which was estimated to be small. We felt that at this stage additional computational effort to treat relaxation of ions around hydrogen was not warranted. Finally, the conclusions are given in Chapter VI.

The theoretical work has been rich in by-products that are not all directly connected with the main topics of this thesis. However, they contain useful information on further applications of the general methods used. These papers are included as appendices in the same form as published or submitted for publication. In the first, Appendix A, the lattice statics formalism is generalized for hexagonal crystals and applied to treat relaxations around a vacancy in magnesium. The second, Appendix B, deals with residual resistivities of alkali impurities in alkali metals and includes the correction due to the relaxation of atoms

around the impurity atom. Exact calculation of the corrections to the residual resistivity due to this lattice relaxation is numerically complicated and may consume considerable computation time. A discussion of different approximate schemes for treating this problem is given in Appendix C. Finally, in Appendix D, a short description of the developed computer programs is supplied.

Except in Chapter II, atomic system of units with $\hbar = m = e = 1$ is used throughout the thesis.

CHAPTER II

MEASUREMENT OF THE SOLUBILITY OF HYDROGEN IN SOLID MAGNESIUM

2.1 Description of the Experimental Method

The solubility of hydrogen in molten magnesium has been investigated by a number of researchers (good reviews are given in Emley 1966 and Mueler et al. 1968). However, in solid magnesium only the solubility just below the melting point (640°C) has been measured (Koeneman and Metcalfe 1959). As one of our major objectives was to determine the heat of solution in solid magnesium, it was necessary to extend the solubility measurements to temperatures at least 200°C below the melting temperature. We have designed an apparatus which directly measures the volume of the gas absorbed at constant pressure, and used it to determine the solubility of hydrogen in magnesium in the temperature interval 400 - 600°C.

When working with magnesium at high temperatures, special precautions have to be taken. In the temperature interval 400°C to the melting point of 650°C the vapour pressure of magnesium varies from about 10^{-2} to 2.75 mmHg. It also reacts chemically with any glass, quartz or Vycor, forming magnesium silicide. Therefore, it was necessary to

reduce the amount of magnesium evaporated and avoid contact of the vapour with Vycor, from which the tube holding the sample has been made. Following Koeneman and Metcalfe (1959), the magnesium samples have been welded into iron containers with a wall less than 0.1 mm thick. With convenient shape of electrodes and overlapping spot welds, it was possible to seal the container completely and avoid leaks of magnesium vapour. Iron does not react with magnesium, has high hydrogen permeability, and due to the small mass of the container the amount of hydrogen absorbed in it is small compared to the amount absorbed in the sample.

A schematic diagram of the apparatus is given in Figure 2.1. The source of hydrogen at constant pressure is a 5 liter bulb which is thermally insulated from the environment to minimize the influence of temperature fluctuations on pressure. The temperature of the bulb was kept at 25 ± 1°C using an electronic controller and an ordinary light bulb as heater. The typical volume of hydrogen absorbed of 3 - 20 cm^3 is small compared to the volume of the bulb, so that the change of pressure due to hydrogen absorption can be neglected. The pressure was measured by a conventional mercury manometer. The part of the apparatus for the measurement of the volume of absorbed hydrogen consists of a mercury drop in a glass tube of length 120 cm and internal diameter 2mm. The volume of gas

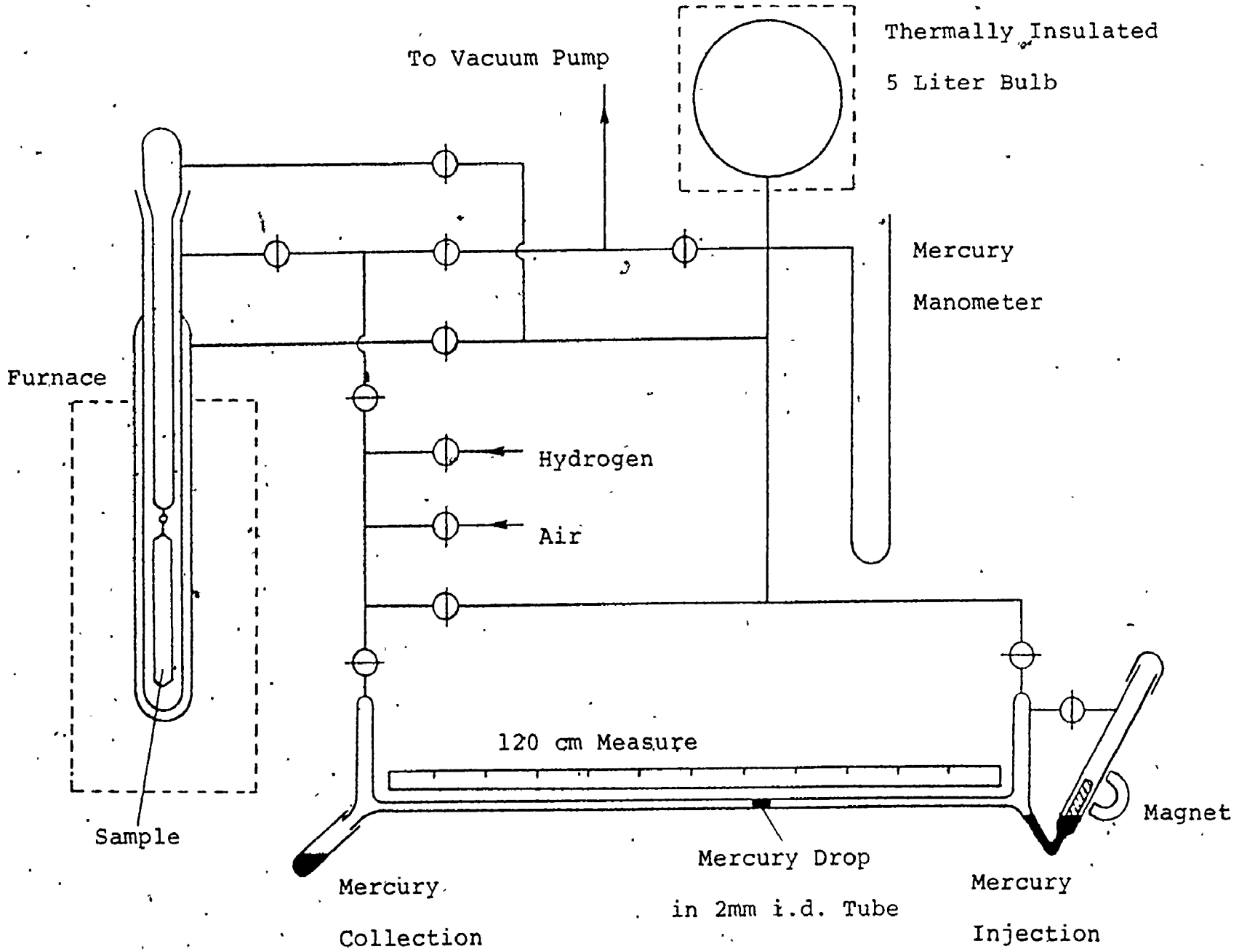

Figure 2.1: Schematic diagram of the apparatus for hydrogen solubility measurements

absorbed is determined by the distance the mercury drop moved during the time of an experiment. The total volume of the measuring tube was about 3 cm^3 but it was also necessary to measure larger volumes. Therefore, a device for injecting mercury drops at one end of the tube was constructed, with the space for mercury collection provided at the opposite end. In this way by injecting a new mercury drop when the old one reached the end of the measuring tube, absorbed volumes greater than 3 cm^3 could be measured. It might be worthwhile to describe the device for mercury injection. As seen from Figure 2.1, it consists of a U-tube filled with mercury on which a glass coated piece of iron floats. Mercury is injected in the measuring tube by moving the float using a small magnet. Two stoppers are provided to refill the system when all available mercury is transferred to the collecting end. The good feature of this simple device is that it does not have any moving parts that could leak gas and it gives a direct measurement of the volume absorbed.

Due to friction, the mercury drop tends to move in jumps rather than continuously as the gas is being absorbed. By attaching a small mechanical vibrator to the measuring tube, the force needed to move the drop is greatly reduced and it moves much more continuously during the course of an experiment.

The quantities of gas we have measured are between 3 and 20 cm^3, depending on pressure and sample temperature. It turned out that the diffusion of hydrogen through the vycor reaction tube in the furnace is significant and cannot be neglected. To solve that problem, a reaction tube with double walls was made. The space between the walls was connected to the hydrogen supply bulb. In this way, diffusion losses from the reaction chamber were prevented, and the small loss of hydrogen through the outside wall, being supplied from the 5 liter bulb can be neglected. The accuracy of measurements also critically depends on the parasitic volume in the measuring system and temperature stability in the furnace. By attaching a long sealed vycor tube to the stopper of the reaction chamber, the parasitic volume has been minimized and utilizing a three-zone furnace with separate temperature control for each zone, a temperature stability of better than 0.5°C has been achieved. Independent temperature control of the three zones was also important for maintaining a temperature gradient which prevented sample deterioration due to continuous magnesium condensation at the cold ends of the iron container. This will be discussed more fully later. For temperature measurements, chromel-alumel thermocouples have been used. The whole apparatus is attached to the vacuum system consisting of a mercury diffusion pump with a cold trap and a mechanical backing pump.

The measuring procedure is as follows. After the sample is introduced into the reaction tube, the whole system is pumped down to a pressure less than 10^{-2} mmHg and filled with commercially available ultra high purity hydrogen gas (99.999% pure) until the desired pressure is reached. Then only the reaction chamber with the sample is degassed for about 10 hours at 600°C until a vacuum better than 10^{-5} mmHg is achieved. After that the reaction chamber is disconnected from the vacuum pump and in a short period of time (1 - 2 sec) hydrogen is introduced from the supply bulb. With the system of stopcocks, the flow of hydrogen being absorbed by the sample is then directed through the measuring tube so that the displacement of the mercury drop directly gives the volume of the gas absorbed at a given pressure. Depending on temperature and pressure, the time necessary to reach equilibrium varied between 1 and 5 hours.

2.2 Results of the Measurements

The measurements have been performed on commercially available high purity magnesium (99.98% pure). This purity was confirmed by residual resistivity measurements at liquid helium temperatures. The value of 0.02 μΩ-cm obtained for the residual resistivity is consistent with the specified

purity if we assume an average contribution from the impurities of 1 μΩ-cm/at %. By optical inspection, a large grain size varying between 2 and 5 millimeters, was observed.

Samples used in the measurement were cylindrical in shape, 1 cm in diameter, 12 cm long, and weighing about 16 grams. The iron container was made to fit the sample as snugly as possible using cold rolled iron sheets of 0.07 mm thickness. With prismatic electrodes and overlapping spot welds, good sealing of the iron container was achieved so that no magnesium vapour reacted with the vycor tube. Special precautions were taken at the ends of the cylindrical containers where spot welding was not possible. The end of a cylinder was squashed together and sealed by welding with a flame. Inevitably, some parasitic volume remained between the magnesium sample and the container. However, this was taken into account when determining solubilities.

In the first couple of measurements attempted, the amount of hydrogen absorbed was much greater than expected and we were not actually able to achieve equilibrium. Careful examination of the sample and container showed condensation of magnesium at the colder container ends, forming a very fine sponge-like material. We suspected that the enormous surface area of such a constantly growing material caused a continual hydrogen absorption. As our furnace had three zones with separate temperature controllers,

it was easy to maintain a temperature gradient where the ends of the container were slightly hotter than the middle of the sample. In this way continual mass transfer was avoided; samples did not deteriorate after 100 - 200 hours at high temperature in the furnace, and the absorbed hydrogen achieved an equilibrium value.

The parasitic volume was estimated by measuring the volume of the container and subtracting the volume of iron and magnesium. It was also corrected for the absorption measured when there was no sample in the reaction tube. The resulting parasitic volume was 1.5 cm^3.

It is generally thought that hydrogen is dissolved in a metal as atoms forming an interstitial solid solution. Then for small concentrations, when hydrogen-hydrogen interactions in a metal are negligible, solubility must follow Sievert's law:

$$S = \text{const} \cdot p^{1/2} \quad . \tag{2.1}$$

The measurements have been performed at five temperatures in the interval 400 - 600°C and at four pressures at each given temperature. The different pressures have been chosen to give equidistant points when the solubility is plotted as a function of $p^{1/2}$. The final measurements at 603°C, 554°C and 503°C were performed on a

sample weighing 16.2 grams. The sample used for 454°C and 403°C measurements weighed 15.6 grams. For both cases parasitic volumes were the same as already mentioned, i.e., 1.5 cm^3.

If v is the measured volume of the gas absorbed at pressure p and v_0 is the parasitic volume, the amount of hydrogen absorbed, measured in cm^3 at normal temperature and pressure (NTP) conditions, is

$$v_H = (v - v_0) \frac{p}{p_0} \frac{273}{298} \quad , \tag{2.2}$$

where 298°K is the hydrogen supply bulb temperature and p_0 is the atmospheric pressure. To get the solubility in units of cm^3 NTP H_2/100 gr Mg, Equation (2.2) has to be multiplied by $100/m_{Mg}$ where m_{Mg} is the mass of magnesium. The solubility can then be written as

$$S = (v - v_0) \frac{p}{p_0} \frac{273}{298} \frac{100}{m_{Mg}} \quad . \tag{2.3}$$

The corrections due to absorption in the steel container can be neglected, being less than 0.03 cm^3 at atmospheric pressure.

The results of the measurements are given in Table 2.1 and Figure 2.2. As seen from the figure, where the solubility is plotted as a function of the square root of pressure, the experimental points lie on straight lines in

TABLE 2.1

RESULTS OF THE MEASURED SOLUBILITIES OF HYDROGEN IN SOLID MAGNESIUM FOR DIFFERENT TEMPERATURES AND PRESSURES

Temperature (°C)	Pressure (mmHg)	Volume Absorbed (cm^3)	Solubility (cm^3 NTP H_2/100 gr Mg)
603	764	5.60	23.0
	447	6.79	17.3
	195	9.40	11.5
	50	17.50	5.8
554	760	4.63	17.4
	446	5.50	13.0
	196	7.89	9.1
	50	14.14	4.7
503	761	3.96	13.6
	446	4.68	10.3
	195.5	6.47	7.1
	50.5	12.15	3.9
454	760	3.25	10.6
	442	3.88	8.4
	199	5.27	6.0
	52	9.67	3.4

TABLE 2.1 - continued

Temperature (°C)	Pressure (mmHg)	Volume Absorbed (cm^3)	Solubility (cm^3 NTP H_2/100 gr Mg)
403	760	2.90	8.5
	444	3.20	6.0
	200	4.16	4.2
	50	7.04	2.2

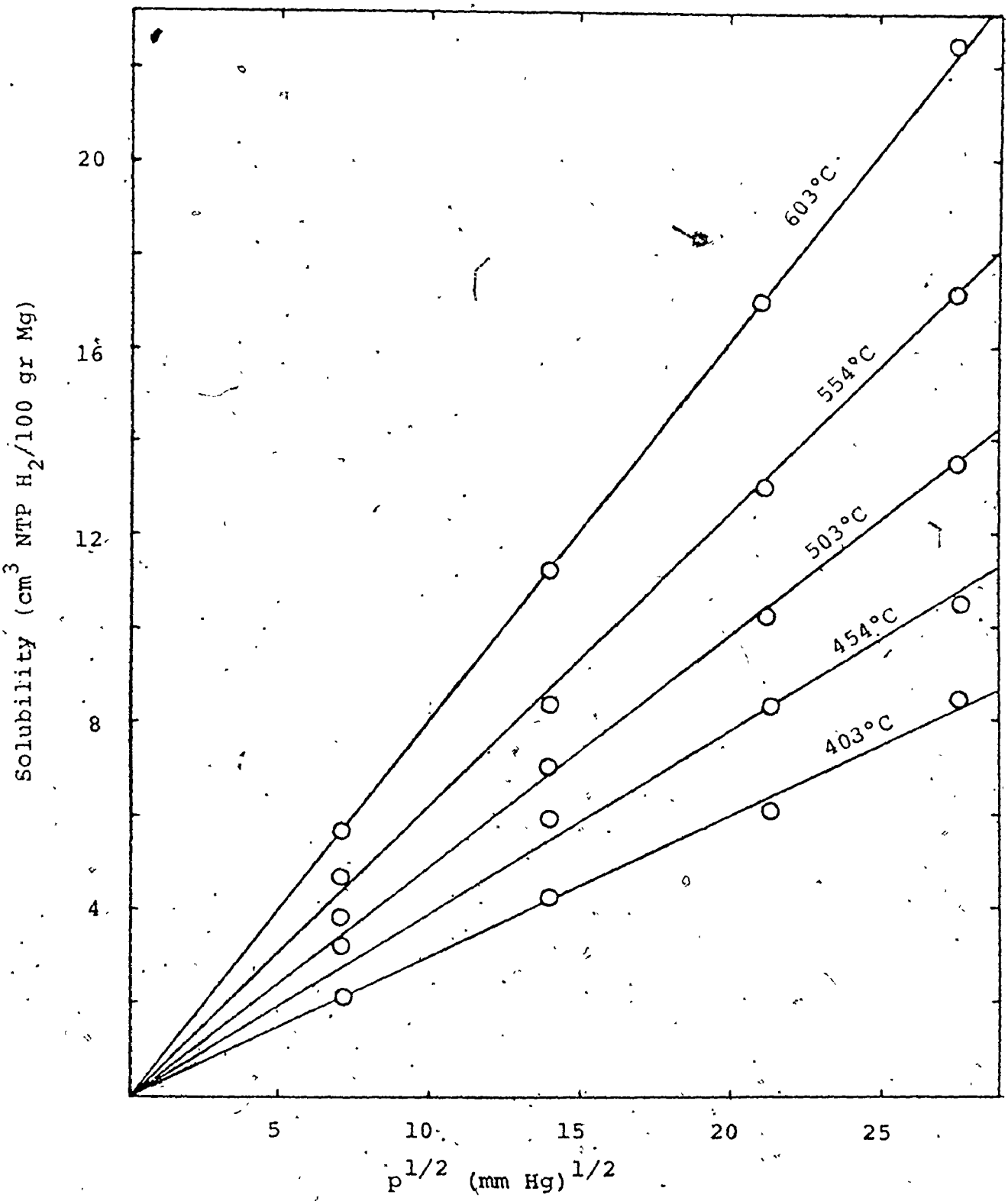

Figure 2.2: Solubility of hydrogen as a function of pressure for different temperatures

accordance with Sieverts' law. Therefore, we can assume that for achieved hydrogen concentrations in solution, pairing of hydrogen atoms is insignificant. The straight lines were obtained by least squares fit and the solubilities corresponding to these lines are plotted using a logarithmic scale in Figure 2.3. The straight line on this figure corresponds again to the least squares fit of the logarithm of solubility versus 1/T. In the temperature and pressure range considered, our experimental results can be well represented with the expression

$$S = 608\left(\frac{p}{p_0}\right)^{1/2} \exp(-5820/RT) \quad , \tag{2.4}$$

where solubility is given in units of cm^3 NTP H_2 per 100 grams of Mg and p_0 is the atmospheric pressure. From Equation (2.2) the solubility at 640°C and atmospheric pressure of 25 cm^3 NTP H_2/100 gr Mg is obtained which is in reasonable agreement with the value of 30 cm^3 NTP H_2/100 gr Mg reported by Koeneman and Metcalfe (1959).

The slope of the logarithmic plot determines the heat of solution. From (2.2) we have ΔH_H = 5820 cal/$\frac{1}{2}$ mole H_2 or ΔH_H = 0.25 eV/atom. The results of our theoretical calculations will be compared with this value.

To check our estimate of the parasitic volume, least squares fits of the experimental data were performed assuming Sieverets' law and taking parasitic volume as an adjustable

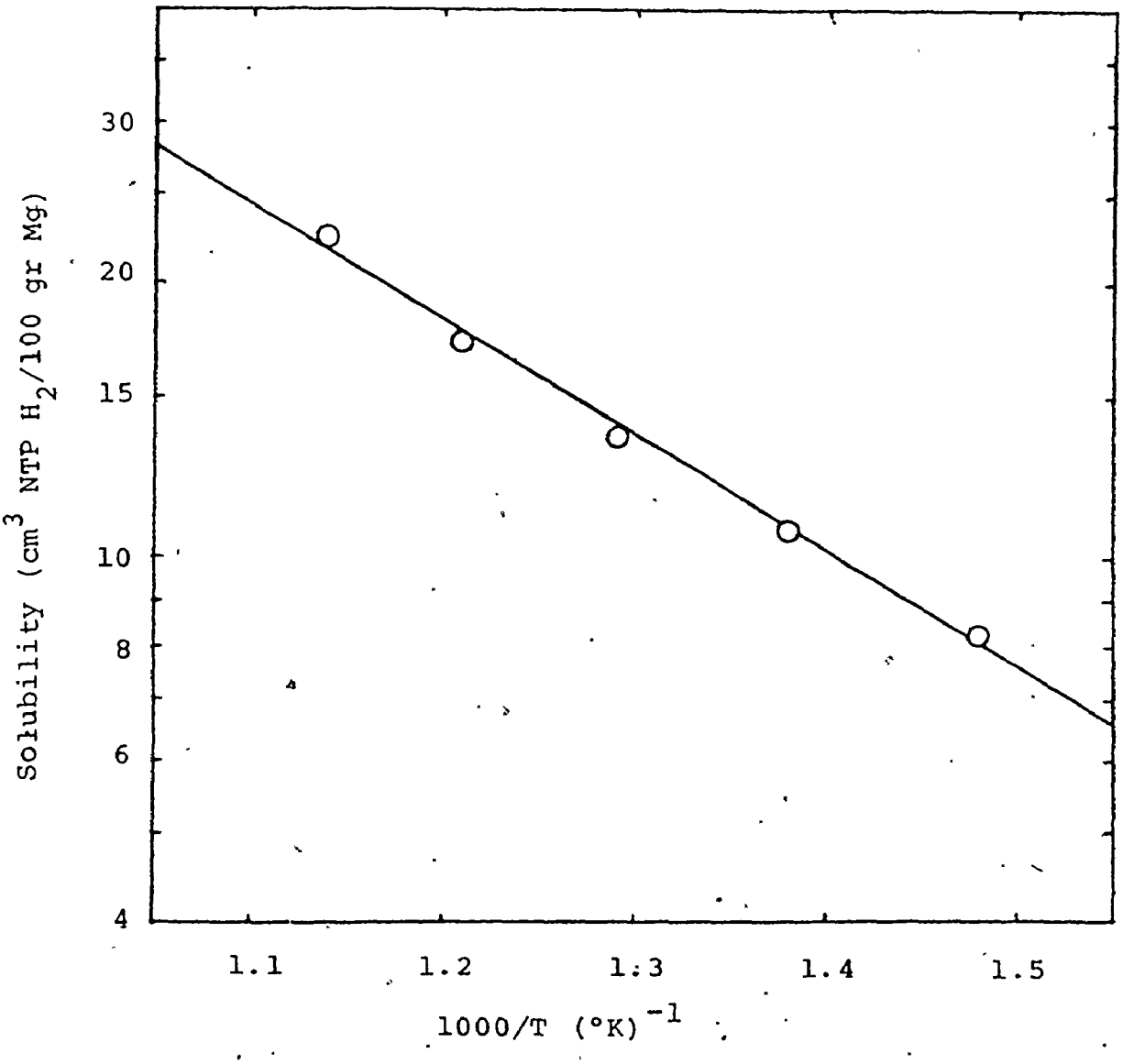

Figure 2.3: Logarithmic plot of the solubility of hydrogen in magnesium versus reciprocal temperature at atmospheric pressure.

parameter. For different measurements, the parasitic volumes thus obtained were between 1.3 and 1.7 cm^3, confirming our estimate of 1.5 cm^3. The discrepancy of $\pm$ 0.2 cm^3 is consistent with the error in volume measurements estimated to be $\pm$ 0.15 cm^3 from temperature fluctuations and friction forces on the mercury drop in the measuring tube. To assess the probable error in the heat of solution, the solubilities have been recalculated using parasitic volumes of 1.3 and 1.7 cm^3. The result obtained:

$$S = (608 \pm 150)\left(\frac{p}{p_0}\right)^{1/2} \exp[-(5820 \pm 500)/RT] \quad , \quad (2.5)$$

gives for the heat of solution of hydrogen the value 5820 $\pm$ 500 k cal/$\frac{1}{2}$ mole H_2 or 0.25 $\pm$ 0.02 eV/atom.

CHAPTER III

REVIEW OF LOCAL PSEUDOPOTENTIAL THEORY

3.1 Basic Ideas of Pseudopotential Theory

In this chapter we will review the basic results of local pseudopotential theory which are necessary for the theoretical treatment of vacancies and hydrogen in metals. We will not try to give a full theoretical justification for the introduction of pseudopotentials. We will rather expose general ideas and quote well known and extensively used formulas which will be the basis of our treatment.

Electrons in a metal can be divided into two groups, valence electrons which are not localized and move freely through the whole metal, and all other electrons which are more or less localized and bound to the individual atomic nuclei. The electrons belonging to the second group are called core electrons and together with the nuclei form ionic cores or simply ions. The essential approximation in all calculations of the properties of metals is the self consistent field assumption. Valence electrons are regarded as independent particles moving in the field of ions and an average field due to all the other electrons. In simple metals, which are the only ones, we will consider, electrons in the ionic core are so strongly bound that we can regard

the core electron states to be the same as in a free atom. Then the metal can be viewed as a regular arrangement of ions immersed in an electron gas. The field of the ionic cores is very strong with a singularity at the nucleus. However, the behaviour of the valence electrons is only influenced by the way they are scattered by the ions and does not depend on the detailed structure of the electron wavefunctions in the region of the ionic cores. The basic idea of pseudopotential theory is to replace the strong ionic potential with a weak potential that will essentially scatter electrons in the same way. As the new potential is weak, perturbation theory can be applied. This new weak potential is called the bare ion pseudopotential and together with the self consistent potential due to all the valence electrons that screen it, gives the complete pseudopotential. The screening based on first order perturbation theory is usually referred to as linear screening because the induced fluctuations of the electron density are linear functions of the self consistent potential.

Pseudopotentials can be calculated from first principles knowing the core electron states (Harrison 1966). However, such calculations are very complicated and not very accurate. Therefore, an alternative approach has been proposed (Abarenkov and Heine 1965). The ionic core potential is represented by a model potential using a simple analytical form with a number of adjustable parameters.

These parameters are then determined to reproduce the properties of the ions (practically, the energies of the valence electrons in a free atom). The potentials obtained are nonlocal, i.e., they depend on energy and the angular momentum quantum number in addition to spacial coordinates. The whole theory of linear screening of these nonlocal potentials can be developed (Heine and Abarenkov 1964, Animalu and Heine 1965, Shaw 1968, 1969). However, the calculations are very involved and further simplifications are desirable for the treatment of more complicated structures such as defects. The theory is greatly simplified if one supposes that the ionic potentials are local, i.e., only depend on spacial coordinates. This additional approximation enables a straightforward application of linear screening theory and simplifies the calculation of the pseudopotential.

The parameters in the local model potential can be found by matching the value calculated for a property with the experimental value, e.g., electrical resistivity, Fermi surface data, elastic constants, etc. The potential defined in such a way is then used to calculate other properties of the metal.

In our calculations we will use local pseudopotential theory with the simplified Heine-Abarenkov model potential

$$V(r) = \begin{cases} -Z/r, & r > R_m \\ -ZD/R_m, & r < R_m \end{cases} \qquad (3.1)$$

where Z is the valence of the metallic ion and the two adjustable parameters are the core radius R_m, and D which determines the depth of the potential well for $r < R_m$. When ions are represented by a simple analytical form as Equation (3.1), they are usually called pseudoions.

For later discussions it will be important to keep in mind the type of boundary conditions used in the calculations. The standard procedure is to assume periodic boundary conditions imposed on a large cubic supercell containing N atoms (Ziman 1972). All the formulas we will give are based on this assumption and the term crystal of N atoms is used in the sense of a supercell with N atoms. For a large number of atoms the calculated physical quantities must not depend on N and it has to drop out from the final expressions.

3.2 Pseudopotential Calculation of the Total Crystal Energy

Using second order perturbation theory, the total energy of the system of pseudoions immersed in an electron gas can be calculated. For a crystal containing N atoms the

result can be written as a sum of three terms (Harrison 1966)

$$V^T = N(ZV_{el} + V_e + V_b) \quad . \tag{3.2}$$

In this expression, V_{el} is the energy per electron of the electron gas plus the average value of electron-ion interaction. It depends only on volume and does not depend on the detailed arrangement of ions. Choosing the analytical form proposed by Pines and Nozieres (1966), V_{el} can be written as

$$V_{el} = \frac{1.105}{r_s^2} - \frac{0.458}{r_s} - 0.0575 + 0.0155 \ln r_s + \sum_{\vec{k}} \langle \vec{k}|w|\vec{k}\rangle \tag{3.3}$$

where

$$4\pi r_s^3/3 = \Omega_0/Z \quad ,$$

and Ω_0 is the atomic volume. For computational convenience in our further derivations, we will regard V_{el} as a function of k_F.

The Fourier transform of the model potential (3.1) is

$$w(q) = -\frac{4\pi Z}{\Omega_0 q^2}\left[D\,\frac{\sin(qR_m)}{qR_m} + (1-D)\cos(qR_m)\right] , \qquad (3.4)$$

and it is called the pseudopotential form factor. Using this pseudopotential the average value of the electron-ion interaction, i.e., the change in energy per valence electron due to the positive charge being in ion cores rather than point charges, is

$$\sum_{\vec{k}} \langle\vec{k}|w|\vec{k}\rangle = \lim_{q\to 0}\left[\frac{4\pi Z}{\Omega_0 q^2} + w(q)\right]$$

$$= \frac{2\pi Z}{\Omega_0} R_m^2\left(1 - \frac{2}{3} D\right) . \qquad (3.5)$$

Introducing the structure factor for the ions,

$$S(\vec{q}) = \frac{1}{N}\sum_{j=1}^{N} e^{-i\vec{q}\cdot\vec{r}_j} , \qquad (3.6)$$

where $\vec{r}_j$ are the position vectors of the ions, the electrostatic energy V_e in (3.2) can be expressed as (Harrison 1966)

$$V_e = \lim_{\xi\to\infty}\left[\sum_{\vec{q}}{}' S(\vec{q})S^*(\vec{q})F_e(q)\right.$$

$$\left. - Z^2\left(\frac{\xi}{\pi}\right)^{1/2} - \frac{\pi Z^2}{2\xi\Omega_0}\right] , \qquad (3.7)$$

where the prime in the summation sign means that the term

$\vec{q} = 0$ is omitted and

$$F_e(q) = \frac{2\pi Z^2}{\Omega_0 q^2} e^{-q^2/4\xi} \quad . \tag{3.8}$$

The last term in (3.2) which is called the band structure energy, can be written as

$$V_b = \sum_{\vec{q}}' S(\vec{q}) S^*(\vec{q}) F_b(q) \quad . \tag{3.9}$$

For a local pseudopotential F_b is given by (Shyu and Gaspari 1968)

$$F_b(q) = -\frac{1}{2} \frac{\Omega_0 q^2}{4\pi} \frac{w^2(q)}{1-f(q)} \left[1 - \frac{1}{\varepsilon(q)}\right] \quad . \tag{3.10}$$

The function $f(q)$, which accounts for exchange and correlation corrections, also appears in the electron dielectric function

$$\varepsilon(q) = 1 + [1-f(q)] \frac{4k_F}{\pi q^2} \cdot \left(\frac{1}{2} + \frac{4k_F^2 - q^2}{8k_F q} \times \ell n \left|\frac{2k_F + q}{2k_F - q}\right|\right) \quad . \tag{3.11}$$

For $f(q)$ we have chosen the analytical form proposed by Singwi et al. (1970)

$$f(q) = A_s[1 - e^{-B_s(q/k_F)^2}] \quad , \qquad (3.12)$$

where A_s and B_s are parameters which depend on the electron density.

The formulae given for total energy are valid for any configuration of ions, i.e., for a perfect crystal as well as for a crystal with defects (vacancies, interstitials, stacking faults). The ionic configuration comes into the energy only through the structure factor (3.6). The electrostatic and bandstructure energies in (3.2) both depend on structure factor and, therefore, on the detailed arrangement of the ions. To calculate the energy of different ionic configurations, it is only necessary to find the corresponding structure factor and use given formulae. In the case when all ions are not the same, the formulae must be slightly modified. This will be done when we treat hydrogen as on interstitial impurity.

3.3 Perfect Crystal

For reasons that will be explained later, we will determine our model potential parameters R_m and D (Equation (3.1)) to reproduce the equilibrium lattice parameter and bulk modulus or binding energy of the perfect crystal. For

a perfect crystal $S(\vec{q})$ (Equation (3.6)) is different from zero only for $\vec{q}$ equal to a reciprocal lattice vector $\vec{q}_0$. The value of $S(\vec{q}_0)$ depends on the type of crystal lattice. For cubic lattices which have one atom per primitive unit cell $S(\vec{q}_0) = 1$. For hexagonal close packed crystals with two atoms per primitive unit cell $S(\vec{q})$ can be represented as a product of the structure factor for the simple hexagonal lattice $S_{sh}(\vec{q})$ and the structure factor of the primitive unit cell

$$S_{hcp}(\vec{q}) = S_{sh}(\vec{q}) \cdot S_u(\vec{q}) \quad , \tag{3.13}$$

with

$$S_u(\vec{q}) = \frac{1}{2} \left(1 + e^{-i\vec{q}\vec{\rho}_2}\right) \quad , \tag{3.14}$$

where $\vec{\rho}_2$ is the position vector of the second atom in the cell and the first atom is at the origin.

The electrostatic energy per ion for a perfect crystal is $\alpha Z^{5/3}/2r_s$, where α is the Ewald constant equal to -1.79186 for bcc, -1.79175 for fcc and -1.79166 for hcp lattices. Using this and Equation (3.13) the total energy of the perfect crystal can be written (using $S_u \equiv 1$ for cubic crystals), as

$$V^T = N \sum_{q_0} S_u^*(\vec{q}) S_u(\vec{q}) F_b(q) + NZV_{el}(k_F) + N \frac{\alpha Z^{5/3}}{2r_s} \quad . \tag{3.15}$$

The physical meaning of V^T is the energy gained when the crystal is formed of N ionized atoms and electrons having zero energy. Reduced to the value per atom, it is the binding energy V_{bind} per atom of a crystal. This quantity is equal to the sum of the ionization potentials of all the valence electrons of the atom and the cohesive energy per atom. Therefore, we can write:

$$V_{bind} = \sum_{q_0} S_u^* S_u F_b + ZV_{el} + \frac{\alpha Z^{5/3}}{2r_s} \quad . \tag{3.16}$$

To find the bulk modulus and the equilibrium lattice condition let us uniformly dilate the crystal by δ. The direct and reciprocal space quantities will then change according to

$$\begin{aligned} r_s &\rightarrow r_s/(1-\delta) \quad , \\ \vec{q} &\rightarrow \vec{q}(1-\delta) \quad , \\ k_F &\rightarrow k_F(1-\delta) \quad . \end{aligned} \tag{3.17}$$

For a given ion pseudopotential, the energy-wave-number characteristics F_b depend on q and on k_F. For

computational convenience we will regard it as a function of q and k_F/q. Then the energy of the dilated crystal will be

$$V^T(\delta) = N \sum_{q_0}' F_b[q(1-\delta), k_F/q] S_u^* S_u + NZV_{el}[k_F(1-\delta)] + N \frac{\alpha Z^{5/3}}{2r_s} (1-\delta) \quad . \tag{3.18}$$

On the other hand, since the crystal for $\delta = 0$ is in equilibrium, the expansion of the energy must have the form

$$V^T(\delta) = V^T(0) + \frac{9}{2} B_m \delta^2 V \tag{3.19}$$

where B_m is the bulk modulus and V is the total volume of the crystal. Comparing the expansion of (3.18) in powers of δ with (3.19) we obtain the equilibrium lattice condition

$$\sum_{q_0}' q \frac{\partial F_b}{\partial q} S_u S_u^* + k_F \frac{\partial ZV_{el}}{\partial k_F} + \frac{\alpha Z^{5/3}}{2r_s} = 0 \tag{3.20}$$

and an expression for the bulk modulus

$$B_m = \frac{1}{9\Omega_0} \left(\sum_{q_0} q^2 \frac{\partial^2 F_b}{\partial q^2} S_u^* S_u + k_F^2 \frac{\partial^2 ZV_{el}}{\partial k_F^2} \right) \quad . \tag{3.21}$$

The equations for the equilibrium lattice condition (3.20), bulk modulus (3.21) and binding energy (3.16), together with the related experimental data will be used to

CHAPTER IV

PSEUDOPOTENTIAL CALCULATION OF VACANCY FORMATION ENERGY AND VOLUME IN ALKALI METALS AND ALUMINUM

4.1 Vacancies and Pseudopotentials - General Discussion

Following ideas originally due to Harrison (1966) attempts have been made to apply pseudopotential theory to the calculation of the vacancy formation energy in aluminum (Chang and Falicov 1971) as well as the formation volume and energy in alkali metals (Ho 1971, 1972).

Before proceeding with the discussion of these papers some general arguments will be presented showing important conditions which calculations of vacancy formation energy must satisfy. We will first prove that the formation energy of a vacancy cannot depend on the formation volume (Chang and Falicov 1971); i.e., for a large crystal, the formation energy is the same under constant volume or constant (zero) pressure conditions. If the energy per atom of a crystal is of order 1 the formation energy of the vacancy will also be of order 1. For the crystal with N atoms and volume V, the formation volume Ω_f will be of the order of the atomic volume $\Omega_0 = V/N$. As the elastic properties of a crystal are

essentially unchanged with the creation of one vacancy, the energy involved in relaxing the lattice by Ω_f is $0.5\ B_m\ (\Omega_f/V)^2 \cdot V \sim B_m\Omega_0/N$ (B_m - bulk modulus), which is of order 1/N and, therefore, negligible. Using this fact, Chang and Falicov (1971) have chosen to use a constant volume condition in their calculations, which enabled them to completely eliminate the electron gas energy and work only with the band structure energy. Although their calculation was essentially correct, they failed to obtain good results for the formation energy of a vacancy in aluminum due to insufficient accuracy of their pseudopotential form factors. On the other hand, since Ho (1971, 1972) wanted to calculate both the formation energy and the formation volume, he could not assume constant volume conditions, and therefore, had to include the electron energy in the calculation. He proposed that the parameters in a simplified Heine-Abarenkov model potential be chosen to reproduce the equilibrium lattice constant and bulk modulus. Such an approach seems to us very reasonable since Mukherjee (1965) has noticed a strong correlation between the monovacancy formation energy, atomic volume and Debye temperature (or equivalently, the elastic properties of the crystal). Recently Tewary (1973) derived this relationship assuming only a pair potential between atoms and neglecting the volume-dependent part of the energy. This suggests that in treating vacancy properties, the

formalism that is used should reproduce the elastic properties of the crystal as well as the equilibrium atomic volume.

Ho's conception of the problem is that the atom from the vacancy must be put on the crystal surface and he is, therefore, led to add a term in the formation energy related to the surface. We will now show that we are dealing with a bulk phenomenon, and therefore, the theory has to be formulated entirely in terms of bulk concepts. There is no way to observe one vacancy in a large single crystal, but rather we observe the average properties due to the large number of vacancies that occupy a small but finite fraction of lattice sites. Let the concentration of vacancies be n_v and the concentration of atoms n_o ($n_o >> n_v$). As an example, let us consider a spherical crystal of radius R, which eventually will become very large. Formally, an atom can be regarded to be on the surface if it is within a layer of some small but finite thickness Δ from the crystal surface. The number of "surface" atoms is $4\pi R^2 n_o \Delta$, and the number of vacancies is $(4\pi/3)R^3 n_v$. The ratio of these two quantities is $3(\Delta/R)(n_o/n_v)$ which vanishes when the crystal becomes very large ($R \to \infty$) (Fumi 1955). In other words the number of surface atoms per vacancy tends to zero and, therefore, we conclude that vacancy formation is a bulk phenomenon. This conclusion may also be reached using

the following physical picture. Suppose that we are taking atoms out of the crystal and putting them on the surface. If in this process we would create a finite number of new surface atoms per vacancy the surface would then contribute to the energy. However, that is not true, because the atoms that have previously been on the surface are now in the bulk, being covered with the atoms taken out of the crystal. Thus the number of the surface atoms has remained essentially unchanged and consequently the surface does not influence the vacancy properties.

Using this fact a derivation of vacancy formation energy and volume will be given which never involves surfaces. The derivation follows very closely Ho's work which undoubtedly represents an important contribution to the field. The results are applied to the calculation of vacancy properties in alkali metals and in aluminum.

4.2 Crystal with a Vacancy

We will now concentrate our attention on the calculation of the energy of a crystal with a vacancy for a fixed crystal volume. Later we will allow for uniform dilation of the crystal, which will enable us to calculate the formation volume.

In accordance with the discussion in the introduction we will obtain the vacancy formation energy as the difference of energies of a crystal with one vacancy and the perfect crystal with the same number of atoms. In pseudopotential theory the arrangement of ions comes into the theory only through the structure factor (3.6).

A convenient way to look at the structure factor for a crystal with a vacancy is to imagine that one atom is removed from the center of a crystal with N+1 atoms. Then, assuming a vacancy at the origin, the structure factor (3.6) can be written as (Chang and Falicov 1971)

$$S_v(\vec{q}) = \frac{N+1}{N} S_p(\vec{q}) - \frac{1}{N} \quad , \tag{4.1}$$

where

$$S_p(\vec{q}) = \frac{1}{N+1} \sum_{j=1}^{N+1} e^{-i\vec{q}\cdot\vec{r}_j} \tag{4.2}$$

is the structure factor of a crystal with N+1 atoms and with atoms relaxed around the origin as if the vacancy was present. If the atoms did not relax around the vacancy, $S_p(\vec{q})$ would be equal to the structure factor of a perfect crystal $S_o(\vec{q})$. The introduction of $S_p(\vec{q})$ is convenient as it will allow the separation of the relaxational part of the energy, which can be calculated separately.

According to Equations (3.2) to (3.9), the energy of a crystal with a vacancy is

$$V_{vac} = \lim_{\xi\to\infty} \{\Sigma'_q S_v^* S_v [F_b(q,k_F'/q) + F_e(q,\Omega_0')] + NZV_{el}(k_F') - N[Z^2(\tfrac{\xi}{\pi})^{1/2} + \frac{\pi Z^2}{2\xi\Omega_0}]\} \quad . \qquad (4.3)$$

In this equation $k_F' = k_F(1 - 1/3N)$ and $\Omega_0' = \Omega_0(N+1)/N$, because, by taking one atom out of the crystal and keeping the volume fixed the density of atoms and electrons has changed. By evaluating the electrostatic energy of a non-relaxed vacancy (Harrison 1966) and taking into account that for the perfect cubic crystal $S_o^2 = S_o = 1$, Equation (4.3) can be written as

$$V_{vac} = E_R + \Sigma'_q [(N - \tfrac{1}{N})S_o + \tfrac{1}{N}]F_b(q,k_F'/q) + NZV_{el}(k_F') + (N-1)\frac{\alpha Z^{5/3}}{2r_s} \quad , \qquad (4.4)$$

where the relaxation energy

$$E_R = \Sigma'_q \frac{1}{N} \{|(N+1)S_p - 1|^2 - |(N+1)S_o - 1|^2\} \times [F_b(q,k_F'/q) + F_e(q,\Omega_0')] \quad , \quad (\xi \to \infty) \qquad (4.5)$$

has been introduced. Obviously $E_R = 0$ for the non-relaxed vacancy because then $S_p = S_o$. The separation of the relaxation energy is very useful because to calculate E_R we can make use of the well-developed and extensively employed lattice statics formalism (Kanzaki 1957, Flocken and Hardy 1969, Appendices A and B).

4.3 Calculation of Formation Energy and Volume of a Vacancy

Periodic boundary conditions, which are used in our calculations, are equivalent to an infinite crystal composed of repeating supercells. In the last section we have obtained the expression for the total energy of a supercell with one vacancy, at fixed volume. This energy can be reduced by dilation of the supercell (Hardy 1968), and from the way we created the vacancy, it is obvious that the formation volume of a vacancy will be given by (Ho 1971)

$$\Omega_f = \Omega_o(1 + 3N\delta) \quad . \tag{4.6}$$

Evidently the dilation δ has to be of order 1/N. Due to the dilation, all vectors in direct and reciprocal space will change according to

$$r_s \to r_s/(1-\delta) \quad ,$$

$$\vec{q} \to \vec{q}(1-\delta) \quad ,$$

$$k_F' \to k_F(1 - 1/3N)(1-\delta) \quad , \tag{4.7}$$

$$k_F'/q \to (k_F/q)(1 - 1/3N) \quad ,$$

where we have included the change of k_F due to the change of electron density in creating the vacancy. The corresponding change in r_s in the electrostatic term has already been taken care of in passing from (4.3) to (4.4).

To minimize the energy of a crystal with a vacancy we will expand V_{vac} to second order in δ. In doing this it is sufficient to retain only terms down to the order 1/N, where E_R and the crystal energy per atom are considered to be of order one. Higher order terms do not contribute to either the formation energy or the formation volume. Substituting (4.7) in (4.4) and using the equilibrium condition (3.20), one obtains after a long but straightforward calculation

$$V_{vac} = V^T + E_f + A\delta + \frac{1}{2} BN\delta^2$$

$$+ \text{terms of the order } 1/N \text{ not containing } \delta \quad , \tag{4.8}$$

where V^T is the energy of the perfect crystal of N atoms and

$$E_f = E_R + \frac{1}{N} \sum_{q}' F_b - \frac{1}{3} \sum_{q_0}' \frac{k_F}{q} \frac{\partial F_b}{\partial (k_F/q)} - \frac{1}{3} k_F \frac{\partial ZV_{el}}{\partial k_F} - \frac{\alpha Z^{5/3}}{2r_s} \quad , \tag{4.9}$$

$$A = \frac{\partial E_R}{\partial \delta} - \frac{1}{N} \sum_{q}' q \frac{\partial F_b}{\partial q} + \frac{1}{3} \sum_{q_0}' k_F \frac{\partial^2 F_b}{\partial q \partial (k_F/q)} + \frac{1}{3} \left(k_F^2 \frac{\partial^2 ZV_{el}}{\partial k_F^2} + k_F \frac{\partial ZV_{el}}{\partial k_F}\right) + \frac{\alpha Z^{5/3}}{2r_s} \quad , \tag{4.10}$$

$$B = \sum_{q_0}' q^2 \frac{\partial^2 F_b}{\partial q^2} + k_F^2 \frac{\partial^2 ZV_{el}}{\partial k_F^2} \quad . \tag{4.11}$$

As discussed in the introduction, the vacancy formation energy cannot depend on the formation volume, i.e., on δ. Our result satisfies this condition. The last two terms in (4.8) are negligible, being of order 1/N, and the vacancy formation energy is given by (4.9). However, these terms have to be retained for the calculation of the formation volume. Clearly V_{vac} will have a minimum for $N\delta = - A/B$ so that following (4.6) the formation volume is

$$\Omega_f = \Omega_o(1 - 3A/B) \quad . \tag{4.12}$$

Atomic relaxations around a vacancy, corresponding to the equilibrium configuration depend on δ. This is

explicitly taken into account in our calculation and is reflected in the appearance of the term $\partial E_R/\partial\delta$ in the quantity A (Equation (4.10)).

When calculating derivatives of $V_{el}(k_F)$ it is important to note that Ω_o in the expression (3.5) for the average value of the electron-ion interaction is connected with k_F through the relation $\Omega_o k_F^3 = 3\pi^2 Z$. Keeping that in mind, the calculation of all the terms in E_f, A and B is straightforward except E_R and $\partial E_R/\partial\delta$. The relaxation energy as defined by (4.5), when expanded to the second order in the displacements, can be written as

$$E_R = \frac{1}{2} \sum_{\substack{i\ell \\ \alpha\beta}} \phi_{\alpha\beta}^{i\ell} u_\alpha^i u_\beta^\ell - \sum_{i\alpha} (F_\alpha^i + \frac{1}{2} \sum_\beta \phi_{\alpha\beta}^{oi} u_\beta^i) u_\alpha^i \quad . \tag{4.13}$$

The force constants $\phi_{\alpha\beta}^{i\ell}$ and the forces on atoms in the non-relaxed positions F_α^i can be expressed as (Kenny et al. 1973)

$$\phi_{\alpha\beta}^{i\ell} = - [K_t \delta_{\alpha\beta} + \frac{r_\alpha r_\beta}{r^2} (K_r - K_t)]_{r=|\vec{r}_i - \vec{r}_\ell| \neq 0} \quad , \tag{4.14}$$

$$\phi_{\alpha\beta}^{ii} = - \sum_{\ell \neq i} \phi_{\alpha\beta}^{i\ell} \quad , \tag{4.15}$$

$$F_\alpha^i = |\vec{r}_i| K_t \quad , \tag{4.16}$$

where the radial and tangential force constants are defined through the interionic potential V(r) (Appendix B, Eq. 14) as

$$K_r = \frac{d^2V(r)}{dr^2} \quad , \tag{4.17}$$

$$K_t = \frac{1}{r}\frac{dV(r)}{dr} \quad . \tag{4.18}$$

The relaxation energy, E_R, and the displacements of the atoms around the vacancy are found by minimizing (4.13) with respect to the displacements. The resulting system of equations

$$\frac{\partial E_R}{\partial u_\alpha^i} = 0 \tag{4.19}$$

is elegantly solved by the lattice statics method (Kanzaki 1957, Flocken and Hardy 1969, Appendices A and B). Using condition (4.19), the relaxation energy (4.13) becomes

$$E_R = -\frac{1}{2}\sum_{\alpha i} F_\alpha^i u_\alpha^i \quad . \tag{4.20}$$

The derivative $\partial E_R/\partial\delta$ is most conveniently calculated by differentiating (4.13) and taking into account the condition (4.19). The result is

$$\frac{\partial E_R}{\partial \delta} = \frac{1}{2}\sum_{\substack{i\ell\\ \alpha\beta}} \frac{\partial \phi_{\alpha\beta}^{i\ell}}{\partial\delta} u_\alpha^i u_\beta^\ell - \sum_{\alpha i}\left(\frac{\partial F_\alpha^i}{\partial\delta} + \frac{1}{2}\sum_\beta \frac{\partial \phi_{\alpha\beta}^{oi}}{\partial\delta} u_\beta^i\right) u_\alpha^i \quad . \tag{4.21}$$

The derivatives of ϕ-s and F-s can be traced back to the derivatives of tangential and radial force constants which are easily calculated for a given pseudopotential.

For the numerical evaluation of (4.21) it is convenient to transform the first sum to reciprocal space and to calculate the second in direct space. After performing a Fourier transformation, (4.21) becomes

$$\frac{\partial E_R}{\partial \delta} = \frac{1}{2N} \sum_{\alpha\beta q} \frac{\partial D_{\alpha\beta}(q)}{\partial \delta} u_\alpha^q u_\beta^q - \sum_{\alpha i} \left(\frac{\partial F_\alpha^i}{\partial \delta} + \frac{1}{2} \sum_\beta \frac{\partial \phi_{\alpha\beta}^{oi}}{\partial \delta} u_\beta^i \right) u_\alpha^i \quad , \tag{4.22}$$

where $D_{\alpha\beta}(q)$ and u_α^q are respectively the dynamical matrix and Fourier transform of the displacements.

Formulae for the radial and tangential force constants K_r and K_t are easily obtained using the defining equations (4.17) and (4.18). For completeness, we will give the expressions for their derivatives

$$\frac{\partial K_t}{\partial \delta} = -3K_t + \frac{2Z^2}{\pi r^2} \int_0^\infty dq\, q \frac{\partial G}{\partial q} \left(\cos qr - \frac{\sin qr}{qr} \right) \quad , \tag{4.23}$$

$$\frac{\partial K_r}{\partial \delta} = -3K_r + \frac{2Z^2}{\pi r^2} \int_0^\infty dq\, q \frac{\partial G}{\partial q} \left(2 \frac{\sin qr}{qr} - 2 \cos qr + qr \sin qr \right) \quad , \tag{4.24}$$

where r is the distance between the atoms and

$$G(q, k_F/q) = -\frac{3\pi q^2}{2Zk_F^3} F_b(q, k_F/q) \quad . \tag{4.25}$$

At this point we would like to contrast our formulae with those given by Ho. As a direct comparison is not straightforward, we will only indicate where the main differences lie. First, Ho has an additional term in the total energy which corresponds to putting an atom at the surface of the crystal. Such a term does not appear in our formulation which deals only with bulk quantities. Second, Ho did not notice that the term in the formation energy that is dependent on the formation volume is actually multiplied by the equilibrium condition (3.19) and hence vanishes identically. A third difference arises because his expansion of the electrostatic and electron energy in powers of δ is not completely consistent. Instead of the change in r_s with δ given by (4.7), he writes $r_s \to r_s(1+\delta)$ thus approximating $(1-\delta)^{-1}$ by $1+\delta$ which is only correct to first order. The expansion is, however, needed to second order (his δ has opposite sign to ours). Finally, while Ho's treatment of the change in the relaxation energy with δ involves some approximations, ours is exact to the second order in the displacements.

Before proceeding to the comparison of experimental and theoretical results, it might be appropriate to clarify that we have really calculated what is measured experimentally. All experiments essentially measure the concentration of vacancies as a function of temperature. Because formation energies of divacancies and interstitials are substantially

larger than that of vacancies, the number of vacancies is usually dominant. Under the assumption of low concentration, the interactions between vacancies can be neglected. Statistical mechanics then predicts that the vacancy concentration is proportional to $\exp(-E_f/k_BT)$. The meaning of E_f is the increase in the crystal energy when one vacancy is introduced, and that is exactly what we have calculated. Therefore, E_f deduced from the slope of the logarithmic plot of concentration versus $1/k_BT$ can be directly compared with our theoretically calculated values. Speaking more strictly the slope is determined by the enthalpy of formation per vacancy $H_f = E_f + p\Omega_f$, but at the atmospheric pressure the second term is negligible.

4.4 Results of Calculations and Discussion

Using the formalism described, the vacancy formation energy and volume have been calculated for the alkali metals as well as for aluminum.

The model potential parameters were determined to match the measured equilibrium lattice constant and bulk modulus. In solving the system of Equations (3.20) to (3.21) for the model potential parameters D and R_m (3.1) the root with closest value to the core radius of the Ashcroft empty core model potential has been chosen.

The lattice relaxation contributions (4.20) and (4.21) were calculated by the lattice statics method with interatomic interactions included up to the eighth nearest neighbours (shell). For the integration over the first Brillouin zone a Gauss integration formula of order 2×5 has been used. Sums in reciprocal space were evaluated up to $q_0 < 10(2\pi/a)$, with good convergence. A trial run for aluminum with $q_0 < 15(2\pi/a)$ gave essentially unchanged results. Parameters used in the calculation, together with theoretical and existing experimental results are given in Table 4.1.

Our results for the vacancy formation energy in the alkalis are in good agreement with values from the existing experiments and are very close to Ho's (1971, 1972), probably because the terms by which our formulae differ from his are small. But in aluminum the extra term that he has included to account for putting an atom on the surface is two times larger than the formation energy itself. That is probably the reason why his attempts with aluminum were unsuccessful (Ho 1972).

For the alkalis, the experimental results for the activation volumes for diffusion are given. It is generally accepted that this volume should be close to the formation volume (Wenzl 1970). Our theoretical results are appreciably lower than Ho's and closer to the existing experimental values.

TABLE 4.1

PARAMETERS USED IN THE CALCULATIONS AND COMPARISON OF THEORETICAL AND EXISTING EXPERIMENTAL FORMATION ENERGIES AND VOLUMES FOR VACANCIES IN ALKALI METALS AND ALUMINUM

Metal	a(Å)	$B_m(10^{11}$ dyn/cm^2)	D	$R_m(1/k_F)$	E_f^{exp}(eV)	E_f^{theor}(eV)	Ω_f^{exp}/Ω_0	$\Omega_f^{theor}/\Omega_0$
Li	3.491	1.325	.3730	.9216	.40[a]	.29	.28[f]	.47
					.34±.04[b]			
Na	4.225	.7528	.3079	1.0133	.39[a]	.41	.41[f]	.42
					.42±.03[c]			
K	5.225	.3657	.5723	1.1975	.39[a]	.35		.37
Rb	5.585	.2825	.7273	1.3115		.31		.37
Cs	6.045	.2127	.8079	1.4030		.29		.35
Al(0°K)	4.031	7.938[h]	.3894	1.2906		.86		.70
Al(300°K)	4.049	7.608[h]	.4042	1.2886	.76[d]	.80	0.62[g]	.69
Al(600°K)	4.081[d]	7.115[h]	.4294	1.2871	.66±.04[e]	.70		.67
Al(900°K)	4.119[d]	6.622[h]	.4591	1.2875		.60		.65

[a] MacDonald (1953)

[b] Feder (1970)

[c] Feder and Charbnau (1966)

[d] Simmons and Balluffi (1960)

[e] McKee et al. (1972)

[f] Hultsch and Barnes (1962), given is the activation volume for diffusion

[g] Emrick and McArdle (1969), given is the formation volume at 420°C

[h] Kamm and Alers (1964), values for bulk modulus at 600°K and 900°K are extrapolated

Strictly speaking, our formalism is valid for absolute zero only. However, we feel that by using high temperature bulk moduli and lattice constants, we determine potentials between atoms correctly in some average sense. If the dynamical contribution to the vacancy properties is small, we might expect that our formalism enables us to study, at least approximately, the influence of temperature on the formation energies and volumes of vacancies. Therefore, for aluminum we calculated the vacancy formation energy and volume using the values of lattice constants and bulk moduli measured at different temperatures. The results of these calculations, which are given in Table 4.1, show that the formation energy decreases as the temperature increases, as one might expect, while the formation volume remains roughly constant. At present, our high temperature theoretical values are the most appropriate to compare with experiments. As seen from the table, the agreement is very good.

It is interesting to note that for aluminum, the lattice relaxation contribution to the formation energy is small (about 4%). Recently DuCharme and Weaver (1972) calculated activation energies for self-diffusion in simple metals. As a part of their calculations, they obtained a formation energy for non-relaxed vacancies in aluminum, which can, therefore, be compared with our results. They quote values for several commonly used pseudopotentials and

find considerable variation with the model potential used. For Shaw's nonlocal energy-wave-number characteristic (Shaw and Pynn 1969), their result is .74 eV (at 0°K) which is in good agreement with experiments and close to our values.

Finally, we should point out that we have also tried Harrison's modified model potential (Cohen and Heine 1970). Although it gave a good value for the formation energy for vacancies in Al (.77 eV at 0°K), it failed to give sensible formation energies in the alkali metals and formation volumes in all the metals considered.

CHAPTER V

THEORY OF THE HEAT OF SOLUTION AND SCREENING OF HYDROGEN IN ALUMINUM AND MAGNESIUM

5.1 Formulation of the Problem

In a sense, hydrogen can be regarded as the simplest possible interstitial impurity. The potential of a hydrogen ion (the proton) is strong but there is nothing that can be done about that as no simpler weak potential can be invented that will have the same scattering properties. We can try to apply the lowest order perturbation theory treating a proton as a point charge with the form factor (Langer and Vosko 1960)

$$w_H(q) = -\frac{4\pi}{\Omega_0 q^2} \quad . \tag{5.1}$$

There is little hope that the results of such a theory can successfully describe the real system. However, the process of dissolving a hydrogen atom in a metal involves two particles, an electron and a proton. Consequently, there are two contributions to the heat of solution. We can have reasonable confidence that the electronic contribution is tractable within the framework of pseudopotential theory.

Therefore, we will first develop a linear screening pseudopotential theory for the heat of solution of hydrogen and later we will correct for nonlinear effects in the terms that depend on the presence of the proton in the metal.

The general arguments given for a vacancy at the beginning of Chapter III are also valid for the heat of solution of hydrogen. First, it will not depend on the change of volume as long as the concentration of hydrogen is small, which is certainly valid for both Al and Mg. Therefore, we can assume constant volume conditions in our calculations. Second, the heat of solution will not depend on the surface. There is a double electrostatic layer at the surface of a metal producing a finite potential drop which is one of the major contributions to the work function (Lang and Kohn 1971). As hydrogen involves two particles of opposite charge, an electron and a proton, the change of energy when both particles cross the surface barrier will be zero, and consequently the heat of solution will not depend on the surface. Using these facts, a linear pseudopotential theory for the heat of solution of hydrogen will be developed in the next section.

The experimental heat of solution that is obtained as the slope of the logarithmic plot of the solubility versus $1/T$ at constant hydrogen gas pressure, is equal to the change of energy of a hydrogen atom dissolved in the metal compared to the energy of the hydrogen atom bound in a hydrogen

molecule. To create a free electron and proton from the hydrogen molecule, we need 2.26 eV per atom to dissociate the hydrogen molecule and then 13.6 eV to ionize a hydrogen atom, which adds up to 15.86 eV per atom. Therefore, the experimental heat of solution will be

$$\Delta H_H = 15.86 + \Delta H_{el-p} \text{ (eV)} \qquad (5.2)$$

where ΔH_{el-p} is the heat of solution of a free electron and a proton in vacuum which we need to calculate.

It should be noted that heats of solution are measured at high temperatures and our calculations are valid for absolute zero. An estimate of the zero point energy of a proton based on uncertainty relations gives the value of 10^{-3} eV indicating that at absolute zero we can neglect proton dynamics and assume a static proton. We will further suppose that a proton is sitting at an octahedral site. Our results for the screened electrostatic potential of a proton will justify this assumption. The nearest neighbour estimate gives a lower energy for a proton at an octahedral site than at a tetrahedral site. We will also neglect lattice relaxations about the proton. In the case of a vacancy in both Al and Mg (Chapter IV, Appendix A) the relaxation energy is about -0.03 eV. Using the screened electrostatic potential of a proton the forces acting on neighbouring ions were estimated. They are of the same order as in the vacancy case

and consequently the relaxation energy cannot be much different. In the first approximation we can neglect it in calculating heats of solution of hydrogen. In further refinements of the theory, it will certainly be desirable to take these effects into account.

5.2 Linear Response Theory of the Heat of Solution of Hydrogen in Simple Metals

When we have hydrogen inside a metal, the formulae of Chapter III cannot be applied directly as all the ions are no longer identical. We will now proceed with the necessary modifications treating Equation (3.2) term by term for the total energy of a crystal.

The total electron energy NZV_{el} in (3.2) will be modified because an additional electron is introduced in the lattice. This changes the number of electrons to NZ + 1 and the Fermi wavevector to

$$k_F' = k_F\left(1 + \frac{1}{3NZ}\right) , \qquad (5.3)$$

so that the total electron energy, after expanding V_{el} to the first order in 1/N becomes

$$V_{el}^{T} = (NZ + 1)V_{el}(k_F')$$

$$= NZV_{el}(k_F) + V_{el}(k_F) + \frac{1}{3} k_F \frac{\partial V_{el}}{\partial k_F} \quad . \qquad (5.4)$$

Note that the average value of the electron-ion interaction (3.5) does not depend on the change of k_F, as the atomic volume per host ion has remained the same. Thus, contrary to the case of a vacancy when we now calculate $\partial V_{el}/\partial k_F$ the term (3.5) should be regarded as constant.

The total electrostatic energy NV_e will change due to the addition of a proton. As we neglect lattice relaxations around the proton, the new total electrostatic energy will be

$$V_e^T = N \frac{\alpha Z^{5/3}}{2r_s} + \frac{\alpha_H Z^{2/3}}{r_s} \quad , \qquad (5.5)$$

where the second term is the Coulomb interaction between a proton and ions with neutralizing uniform negative background. It can be calculated by Ewald's method. Using the formulae given by Tosi (1964), and assuming the proton occupies an octahedral site, we have obtained for the constant α_H the value -0.42586 for an fcc and -0.42732 for hcp lattice.

To introduce the necessary modifications in the total band structure energy NV_b, we will rewrite (3.9) in the following form

$$NV_b = \frac{1}{N} \sum_q{}' \, W(\vec{q}) W^*(\vec{q}) g(q, k_F/q) \quad , \tag{5.6}$$

where

$$g(q, k_F/q) = - \frac{1}{2} \frac{\Omega_0 q^2}{4\pi} \frac{1}{1 - f(q)} \left[1 - \frac{1}{\varepsilon(q)}\right] \quad , \tag{5.7}$$

and

$$W(\vec{q}) = NS(\vec{q}) w(q) \quad . \tag{5.8}$$

If we now note that $W(\vec{q})$ is the Fourier transform of the total bare potential and accept that all the ions need not necessarily be of the same kind, the total band structure energy of the lattice with the proton will be given by modifying (5.6) to

$$V_b^T = \frac{1}{N} \sum_q{}' \, W_1(\vec{q}) W_1^*(\vec{q}) g(q, k_F'/q) \quad , \tag{5.9}$$

where

$$W_1(\vec{q}) = NS(\vec{q}) w(q) + w_H(q) e^{-i\vec{q}\vec{\rho}_H} \tag{5.10}$$

is the Fourier transform of the bare potential of all the ions and the proton whose position vector is $\vec{\rho}_H$. The proton form factor $w_H(q)$ is given by (5.1) and we have also taken into account the change of Fermi wavevector to k_F' (Equation (5.3))

due to introduction of an additional electron.

For an hcp crystal $\vec{\rho}_2$ in (3.14) can be chosen in such a way that the position vector of the proton sitting at an octahedral site is

$$\vec{\rho}_H = \frac{1}{2}\vec{\rho}_2 \quad . \tag{5.11}$$

Substituting (5.10) into (5.9), expanding $g(q, k_F'/q)$ to the first order in 1/N, and writing the structure factor using (3.13) and (3.14), we obtain for hcp crystals after a short calculation

$$V_b^T = N \sum_{q_0}' S(\vec{q})S^*(\vec{q})F_b(q) + \frac{1}{2}\sum_{q_0}' \cos^2\frac{1}{2}\vec{q}\vec{\rho}_2 \frac{k_F}{q}\frac{\partial F_b}{\partial(k_F/q)}$$

$$+ \sum_{q_0}' ww_H g(q, k_F/q)\, 2\cos\vec{q}\vec{\rho}_H + \frac{1}{N}\sum_{q}' w_H^2(q)g(q, k_F/q) \quad . \tag{5.12}$$

For fcc crystals the result has the same form with $\vec{\rho}_2 = 0$.

Adding up Equations (5.4), (5.5) and (5.12), and subtracting the total energy of the perfect crystal (3.2), we arrive at the expression for the heat of solution of ionized hydrogen

$$\Delta H_{el-p} = \Delta H_1 + \Delta H_2 \tag{5.13}$$

where

$$\Delta H_1 = V_{el}(k_F) + \frac{1}{3} k_F \frac{\partial V_{el}}{\partial k_F} + \frac{\alpha_H Z^{2/3}}{r_s}$$

$$+ \frac{1}{3} \sum_{q_0} \cos^2 \frac{1}{2} \vec{q}\vec{\rho}_2 \frac{k_F}{q} \frac{\partial F_b}{\partial (k_F/q)} \qquad (5.14)$$

depends only on the properties of the perfect crystal and

$$\Delta H_2 = \sum_{q_0}' w w_H g(q, k_F/q) 2 \cos \vec{q}\vec{\rho}_H + \frac{1}{N} \sum_{q}' w_H^2 g(q, k_F/q) \qquad (5.15)$$

depends on the presence of the proton through the form factor $w_H(q)$.

For the vacancy calculations, the model potential parameters were determined to reproduce the equilibrium lattice condition and the bulk modulus.

For calculating the hydrogen heat of solution, it is more appropriate to determine the parameters to reproduce the binding energy of the crystal (3.16) rather than the bulk modulus, because we are now more interested in correctly calculating the energies of atoms and electrons relative to the vacuum level than in calculating interactions of ions. The relevant experimental data and calculated values of the model potential parameters are given in Table 5.1 (V_{bind} was calculated from ionization potentials and enthalpies of formation taken from Handbook of Chemistry and Physics 1970).

TABLE 5.1

Metal	a (Å)	c/a	V_{bind} (a.u.)	$R_m(1/k_F)$	D
Al	4.031	-	-2.082	1.2847	0.3969
Mg	3.193	1.624	-0.885	1.2270	0.4507

For aluminum, the new model potential parameters are very close to those calculated by reproducing the bulk modulus (Table 4.1). For magnesium, we also calculated the parameters needed to reproduce the bulk modulus. They were found to be somewhat different from those quoted in Table 5.1. We believe that the reason for this difference is due to the somewhat larger ionic core of the Mg ions and also due to more pronounced nonlocal effects in magnesium.

The hydrogen heat of solution calculated from formulae (5.2) and (5.13) to (5.15) with the model potential parameters of Table 5.1 are quoted together with the results of the nonlinear theory in Table 5.5, page 86. We see that the linear theory is inadequate giving values that are too large. It also predicts incorrectly that the heat of solution in magnesium is larger than in aluminum.

Linear theory seriously underestimates terms contributing to ΔH_2, while ΔH_1 is essentially correct because it does not depend on the proton screening. In order to obtain better agreement between theory and experiments, it is essential to go beyond the linear theory in treating the screening of the proton. A self-consistent nonlinear theory of proton screening will be developed in the next section and applied to a more careful treatment of the hydrogen heat of solution.

5.3 Nonlinear Theory for the Screening of a Proton in a Uniform Electron Gas

To be able to compute better values for the term ΔH_2, (Equation (5.15)) which enters the heat of solution of hydrogen in metals and which depends explicitly on the screening of the proton, we need to find the correlation energy of a proton (defined as the change of energy when the proton is introduced in a uniform electron gas), and the electron density in the screening cloud. The theoretical foundation of the method we will use to treat nonlinear screening of a proton has been given by Hohenberg and Kohn (1964) and Kohn and Sham (1965), and is usually referred to as the density functional formalism. In this section we will present the basic results of the theory in a form convenient for attac[illegible] our

The basic theorem of the density functional formalism states that there exists a one body local potential $V_{eff}(\vec{r})$ which through the one body Schroedinger equation

$$[\frac{1}{2}\nabla^2 + V_{eff}(\vec{r})]\psi_i(\vec{r}) = \varepsilon_i\psi_i(\vec{r}) \tag{5.16}$$

generates the set of wavefunctions $\psi_i(\vec{r})$ and the exact ground state density of the system through the independent particle expression

$$n(\vec{r}) = \sum_{\varepsilon_i<\mu} |\psi_i(\vec{r})|^2 \tag{5.17}$$

where μ is the chemical potential of the electrons. It is convenient to express the potential $V_{eff}(\vec{r})$ as

$$V_{eff}(\vec{r}) = V(\vec{r}) + V_{xc}(\vec{r}) \tag{5.18}$$

where $V(\vec{r})$ is the total Coulomb potential

$$V(\vec{r}) = V_{ext}(\vec{r}) + \int \frac{n(\vec{r}')}{|\vec{r}-\vec{r}'|}\, d\vec{r}' \tag{5.19}$$

and $V_{xc}(\vec{r})$ is the functional derivative of a universal exchange and correlation energy functional $E_{xc}[n]$ of the electron density n:

$$V_{xc}(\vec{r}) = \delta E_{xc}[n]/\delta n(\vec{r}) \quad . \qquad (5.20)$$

The main difficulty in a practical application of the theory is that the functional $E_{xc}[n]$ is not known, and various approximations have been proposed for the calculation of the exchange and correlation potential $V_{xc}(\vec{r})$. For a slowly varying density, it can be approximated by the exchange and correlation part of the chemical potential for a uniform electron gas calculated for the local electron density:

$$V_{xc}(\vec{r}) \approx \mu_{xc}[n(\vec{r})] = \varepsilon_{xc} + n \left.\frac{d\varepsilon_{xc}}{dn}\right|_{n=n(\vec{r})} , \qquad (5.21)$$

where ε_{xc} is the exchange and correlation energy of the uniform electron gas. We will use this approximation with the form of μ_{xc} proposed by Hedin and Lundqvist (1971)

$$\mu_{xc}(r_s) = - 0.02909\left[\frac{21}{r_s} + 0.7734 \ln\left(1 + \frac{21}{r_s}\right)\right] , \qquad (5.22)$$

which is based on the work of Singwi et al. (1970). Although near the proton the density is certainly not slowly varying, in using (5.22) for the exchange and correlation potential we do not expect to make a significant error as the effective potential near the proton is dominated by the Coulomb contribution.

Let us now apply Equations (5.16) to (5.19) to the case of a proton in an electron gas. As our problem is

spherically symmetric (5.16) becomes the usual radial Schroedinger equation

$$[-\frac{1}{2}\frac{d^2}{dr^2} + V_{eff}(r) + \frac{\ell(\ell+1)}{r^2} - \varepsilon_\kappa]rR_{\ell\kappa}(r) = 0 \quad , \quad (5.23)$$

where $R_{\ell\kappa}(r)$ is the radial electron wavefunction with the angular momentum quantum number ℓ and κ labeling the electronic states. For nonlocalized states $\varepsilon_\kappa = k^2/2$ where k is the electron wavevector. We cannot exclude the possibility that there will also exist bound states with energies $\varepsilon_b < 0$. The results of our calculations show that only s-type bound states appear and we will denote the corresponding radial wavefunction as $R_b(r)$.

As we know that at large distances the proton potential must be completely screened and $rV_{eff}(r \to \infty) \doteq 0$ the radial wavefunctions of the nonlocalized states when properly normalized must have the asymptotic form well known from the partial wave analysis

$$R_{\ell\kappa}(r) = \cos \eta_\ell j_\ell(\kappa r) - \sin \eta_\ell n_\ell(\kappa r) \quad , \quad (5.24)$$

where the phase shifts η_ℓ depend on κ, and j_ℓ and n_ℓ are the spherical Bessel functions of the first and the second kind respectively. For the possible bound state the asymptotic form must be

$$rR_b(r) \sim e^{-\kappa_0 r} \tag{5.25}$$

with $\kappa_0 = \sqrt{-2\varepsilon_b}$.

What we want to calculate is the induced change of electron density due to the introduction of a proton. Taking into account that when the proton is not in the electron gas, the electron wavefunctions are $j_\ell(\kappa r)$, the change of the electron density calculated from (5.19) is

$$\begin{aligned}\Delta n(r) &= \sum_{\varepsilon_i<\mu} |\psi_i|^2 - n_0 \\ &= \frac{1}{\pi^2}\int_0^{k_F} \kappa^2 d\kappa \sum_{\ell=0}^{\ell_{max}} (2\ell+1)\left[|R_{\ell\kappa}(r)|^2 - |j_\ell(\kappa r)|^2\right] \\ &\quad + 2|R_b(r)|^2 \quad .\end{aligned} \tag{5.26}$$

Due to the spherical symmetry of the problem, the angular parts of the wavefunctions (spherical harmonics) summed over the magnetic quantum number m give a constant. Therefore, it is enough to consider only the radial wavefunctions $R_{\ell\kappa}(r)$. The bound state wavefunction being of s character is equal to the radial function $R_b(r)$. In (5.26) the sum over angular momentum quantum number ℓ should go to infinity ($\ell_{max} \to \infty$). However, as the screened potential of a proton is localized, high ℓ radial functions will be little effected because the potential in (5.23) will

dominated by the centrifugal term $\ell(\ell+1)/r^2$. We have truncated the sum by putting $\ell_{max} = 6$. The phase shifts η_6 are very small (of the order 10^{-4}) so that we do not expect appreciable error from neglecting the changes in the wavefunctions with ℓ higher than 6.

In constructing the electron density we occupy every single electron state with two electrons, one with spin up and the other with spin down. Therefore, our formalism is not capable of treating a single electron bound to the proton. This point will be discussed more fully later.

When we know the change of the electron density $\Delta n(r)$, the Coulomb potential (5.19) can be expressed as

$$V(r) = -\frac{Z_p}{r} + \frac{1}{r}\int_0^r 4\pi r'^2 \Delta n(r')dr' + \int_r^\infty 4\pi r' \Delta n(r')dr' \quad , \tag{5.27}$$

where Z_p is the proton charge and the spherical symmetry of the problem has been used. To make the effective potential equal to zero at infinity, we will redefine the exchange and correlation potential (5.22) as

$$V'_{xc}(r) = \mu_{xc}[n_0 + \Delta n(r)] - \mu_{xc}(n_0) \tag{5.28}$$

so that now the effective potential is

$$V_{eff}(r) = V(r) + V'_{xc}(r) \quad , \tag{5.29}$$

with $V'_{xc}(r)$ given by (5.28).

In order to have complete screening of the proton, the total charge density in the screening cloud must be equal to the charge of the proton. Using phase shifts, this condition can be conveniently expressed in the form

$$Z_p = \frac{2}{\pi} \sum_{\ell=0}^{\ell_{max}} (2\ell+1)\eta_\ell(k_F) \qquad (5.30)$$

which is the well known Friedel sum rule. As mentioned earlier, sufficient accuracy is achieved if we put $\ell_{max} = 6$.

The density functional formalism also leads to an expression for the total energy of the system in terms of the density. However, we are interested in the change of the energy of the ground state when the proton is introduced. This is of the order $1/N_{el}$, where N_{el} is the total number of electrons. Instead of trying to extract this small energy from the total energy, we will use the well known theorem which gives the change of the energy of the system as an integral over the coupling constant (Fetter and Walecka 1971). If we are able to find the interaction energy of a proton with the electron gas $V_{int}(Z_p)$ when the proton charge is changing from 0 to 1, the correlation energy of a proton V_p can be calculated as

$$V_p = \int_0^1 V_{int}(Z_p) \frac{dZ_p}{Z_p} \qquad (5.31)$$

The interaction energy $V_{int}(Z_p)$ is simply the Coulomb interaction energy between a proton and the screening cloud. If we find the change of electron density $\Delta n(r, Z_p)$ for Z_p between 0 and 1, $V_{int}(Z_p)$ will be

$$V_{int}(Z_p) = - Z_p \int_0^\infty 4\pi r' \Delta n(r', Z_p) dr' \quad . \tag{5.32}$$

For nonlinear screening of the proton, the self-consistent induced charge densities should be found satisfying Equations (5.23) to (5.29), for the values of Z_p in the interval 0 to 1. Then, the correlation energy of a proton is calculated using (5.31) and (5.32), and the real induced electron density change $\Delta n(r)$ is the one obtained for $Z_p = 1$.

The scheme we have described can be viewed as a simple nonlinear self-consistent Hartree calculation with approximate corrections for exchange and correlation. By approaching the problem from the point of view of the density functional formalism, we have placed the calculation scheme on firmer theoretical ground. Density functional formalism is in principle an exact theory and also gives a guide to how correlation and exchange corrections should be included. The formalism described without exchange and correlation corrections has been used to treat the nonlinear screening of a fixed point impurity of the charge $Z = \pm 1$ (Sjölander and Stott 1972). For the negative point impurity,

reasonable self-consistent solutions have been achieved. The positive fixed point impurity (which corresponds to the case of the proton) turned out to be a more difficult problem and they did not succeed in obtaining a satisfactory self-consistent solution.

The only other attempt to treat proton screening by solving the Schroedinger equation that we are aware of, has been given by Friedel (1952) who treated a proton in copper. His starting point was a proton with one bound electron with a Slater exchange correction included only for the bound electron and with no correlation correction. In this picture electrons with spins parallel to that of the bound electron feel a more attractive potential from those with antiparallel spin. This allows the occurence of a single bound state. Using an estimate to correct for the presence of the ions, Friedel also calculated the energy of solution of a hydrogen atom in copper, which when added to the dissociation energy of a hydrogen molecule of 2.26 eV gives a heat of solution of 0.2 eV. This value is in reasonable agreement with the recent experimental value of 0.57 eV (McLellan 1973). However, we have some doubts about Friedel's procedure. He calculated the wavefunction of the bound electron in the field of the proton and the remaining screening charge in the Fermi gas. If that is done, the screening is not properly taken into account because due to an electron charge being subtracted from the screening cloud, at large distances the

bound electron would feel the bare Coulomb potential which is certainly not satisfactory.

As mentioned before, our formalism is capable of treating only two bound electrons or none, as it does not distinguish between spin up and spin down electrons. However, it would certainly be desirable as a further refinement of the theory to investigate whether or not self-consistent screening with one bound electron exists and if it has lower energy than the state with two bound electrons. In the following section we will propose a scheme for an approximate self-consistent solution of the proton screening problem. At present we do not see clearly whether this scheme can be applied to the investigation of proton screening with one bound electron.

5.4 Approximate Self-Consistent Solution of Nonlinear Proton Screening

The formalism we have described in the previous section is very similar to the Hartree type calculations successfully used for atoms. As is well known these methods converge well. If we start with a reasonable trial function, after a few iterations good self-consistency is achieved. Why is it then more difficult to solve the similar problem for the electron gas? The answer to this question lies in the

conservation of the number of particles and complete screening at large distances. In the case of an atom, it is automatically satisfied because the number of particles is definite. In the electron gas case, we work with an infinite number of particles in an infinite system. The Friedel sum rule (5.30) which is the condition of complete screening ($rV \to 0$, $r \to \infty$) now plays the role of particle conservation. However, the trouble is that it is not automatically satisfied. If the trial potential does not satisfy the Friedel sum rule, screening will not be complete and the new potential that is generated will be useless because it will have an incorrect behaviour $V \sim 1/r$ at large distances. It might appear appealing to work with a constant number of particles as in the case of atoms and treat a definite large number of electrons in a spherical box. March and Murray (1960) have done such calculations for the screening of a pseudoion, without trying to achieve self-consistency. They concluded that it is necessary to work with a very large number of particles (10^6 or more) in order to make effects due to the box boundary conditions small. There is also no guaranty that a procedure convergent for say 100 particles is also convergent for one million particles, and therefore, we decided to treat the infinite system which is numerically much simpler.

We have tried to achieve full self-consistency by starting with a one parameter trial potential

$rV_{eff} = rV_{trial}(r,a) = \exp(-ar)$. The first step was to determine the parameter a so that the Friedel sum rule was satisfied. Using formulae (5.23) to (5.29), the new potential was generated and renormalized so that the Friedel sum rule was again satisfied. Unfortunately this procedure was not convergent and in successive iterations, the violation of the Friedel sum rule was increasing. Therefore, we started searching for a method that would give satisfactory although approximate self-consistency. It turned out that good self-consistency can be achieved by introducing a two parameter trial function, $V_{trial}(r,a,b)$, and determining the parameters a and b so that the Friedel sum rule is satisfied by both the initial and the newly generated potential $V_{eff}(r)$. We have tried a number of analytical forms and they all gave similar results. For different trial functions, we found that the correlation energies of a proton would not differ by more than 0.5% which is less than 0.1 eV. We found that the trial function of the form

$$rV_{trial}(r,a,b) = \exp(-ar^b) \tag{5.33}$$

is the most flexible, as it is possible to determine the parameters a and b which will produce correct Friedel sum rules for any value of Z_p between 0 and 1, with or without the inclusion of exchange and correlation corrections. The other forms tried could not be used in all the cases.

Let us now describe systematically and in some detail the computational procedure. We start with the trial potential (5.33) with a fixed value for b. The parameter a is calculated so that the Friedel sum rule is satisfied. The Schroedinger equation (5.24) is solved numerically in steps of .05. We suppose that the potential is negligibly small for $r > 10$. As the potential has a singularity at $r = 0$, it is necessary to find a power series solution for small distances and then proceed with the numerical integration. At $r = 10$ the numerical solution is matched to the asymptotic solution (5.24) and the phase shift found. The asymptotic solution is later used for distances between $r = 10$ and $r = 20$. To calculate the electron density in the screening cloud (5.26) we need to find radial wavefunctions for $0 \leq k \leq k_F$. For the integration over k a Gauss integration formula of the 48'th order is used and the sums over ℓ are truncated putting $\ell_{max} = 6$. A bound state appears for $\eta_0 \to \pi$ when $k \to 0$ and it must be included in the screening cloud. It can be found by integrating the Schroedinger equation and determining $\epsilon_b < 0$ in such a way that for $r > 10$, where we suppose $V_{eff} = 0$, the solution matches the asymptotic form (5.25). Once the screening density is known, (5.27) gives the total Coulomb potential and (5,28) and (5.29) the new effective potential. The Friedel sum is calculated for the new effective potential and the whole procedure repeated with

the changed value of the parameter b in (5.33) until the newly generated potential gives the desired Friedel sum.

Values of the parameters a and b determined in this way for different values of Z_p, together with electron-proton Coulomb interaction energies and resulting proton correlation energies are given in Tables 5.2 and 5.3 for Al and Mg respectively. In integrating Equation (5.31) for the proton correlation energy, the five point Lagrange integration formula has been used. We see that for both Al and Mg nonlinear screening dramatically changes the proton correlation energy. Exchange and correlation corrections play an important role giving considerably lower energies than simple Hartree type calculations, and when included a bound state appears in both metals. Hartree screening did not give a bound state for Al but a very shallow bound state appeared for Mg. When exchange and correlation corrections are included, the energies of bound states are approximately 0.005 a.u. for Mg and 0.0005 a.u. for Al. In the case of Mg, the bound state charge density contributes 30% of the total charge density at the proton site (r = 0), while in Al the contribution is only about 10%. This indicates a spatially larger bound state in Al compared to Mg. At still higher electron gas densities (smaller r_s) we expect the bound state to merge with the conduction band and to disappear. The occurence of the bound state has an

TABLE 5.2

RESULTS OF CALCULATIONS OF THE PROTON CORRELATION ENERGY IN Al (r_s = 2.064)

Z_p	Trial Potential Parameters a	b	Interaction Energy V_{int}/Z_p Linear Theory	Nonlinear (Hartree)	Nonlinear (exch + corr)
0.25	1.1014	1.0243	-	-0.1944	-
	0.8987	1.3484	-	-	-0.2203
0.50	1.1591	1.0009	-	-0.4231	-
	0.9870	1.2900	-	-	-0.4864
0.75	1.2188	0.9771	-	-0.6943	-
	1.0747	1.2288	-	-	-0.8066
1.00	1.2726	0.9542	-	-1.0160	-
	1.1530	1.1709	-	-	-1.1857
Proton Correlation Energy V_p			-0.4008	-0.4514	-0.5222

TABLE 5.3

RESULTS OF CALCULATION OF THE PROTON CORRELATION ENERGY IN Mg (r_s = 2.642)

Z_p	Trial Potential Parameters a	b	Interaction Energy V_{int}/Z_p Linear Theory	Nonlinear (Hartree)	Nonlinear (exch + corr)
0.25	0.9685	1.0423	-	-0.1680	-
	0.6647	1.6303	-	-	-0.2006
0.50	1.0459	1.0084	-	-0.3734	-
	0.8111	1.4846	-	-	-0.4553
0.75	1.1234	0.9755	-	-0.6273	-
	0.9487	1.3548	-	-	-0.7745
1.00	1.1968	0.9427	-	-0.9374	-
	1.0630	1.2371	-	-	-1.1569
Proton Correlation Energy V_p			-0.3436	-0.4055	-0.4974

important effect on the proton screening calculations that use perturbation theory based on a free electron gas. As suspected by Sjölander and Stott (1972), they could not adequately treat proton screening, because they inherently cannot produce a bound state.

In Table 5.4 phase shifts at the Fermi level are given for the calculation which included exchange and correlation corrections. For both Mg and Al the rapid decrease of phase shift with increasing angular quantum number ℓ is evident.

Nonlinear results for the proton correlation energy indicate that the electrons are much more strongly localized around the proton than linear theory predicts. It is certainly interesting to see the details of the screened potential as this determines the effect of hydrogen on host ions and other solute ions. On Figures 5.1 and 5.2 the electrostatic potentials multiplied by distance - $rV(r)$ are given for different screening theories. We see that for the full nonlinear theory the potential drops much faster than in the linear case, and the nonlinear Hartree theory gives a potential between these two. At larger distances there is a difference in phase of the wiggles of roughly a quarter of a period, which is very important for the correct calculation of the interaction between the proton and other ions. This phase difference is the characteristic feature of nonlinear screening and has its origin in the phase shifts that are

TABLE 5.4

PHASE SHIFTS AT THE FERMI LEVEL FOR

PROTON IN Al AND Mg

	η_0	η_1	η_2	η_3	η_4	η_5	η_6
Al	1.08127	.12098	.01958	.00334	.00049	.00012	.00003
Mg	1.27190	.07956	.00945	.00117	.00001	.00022	.00018

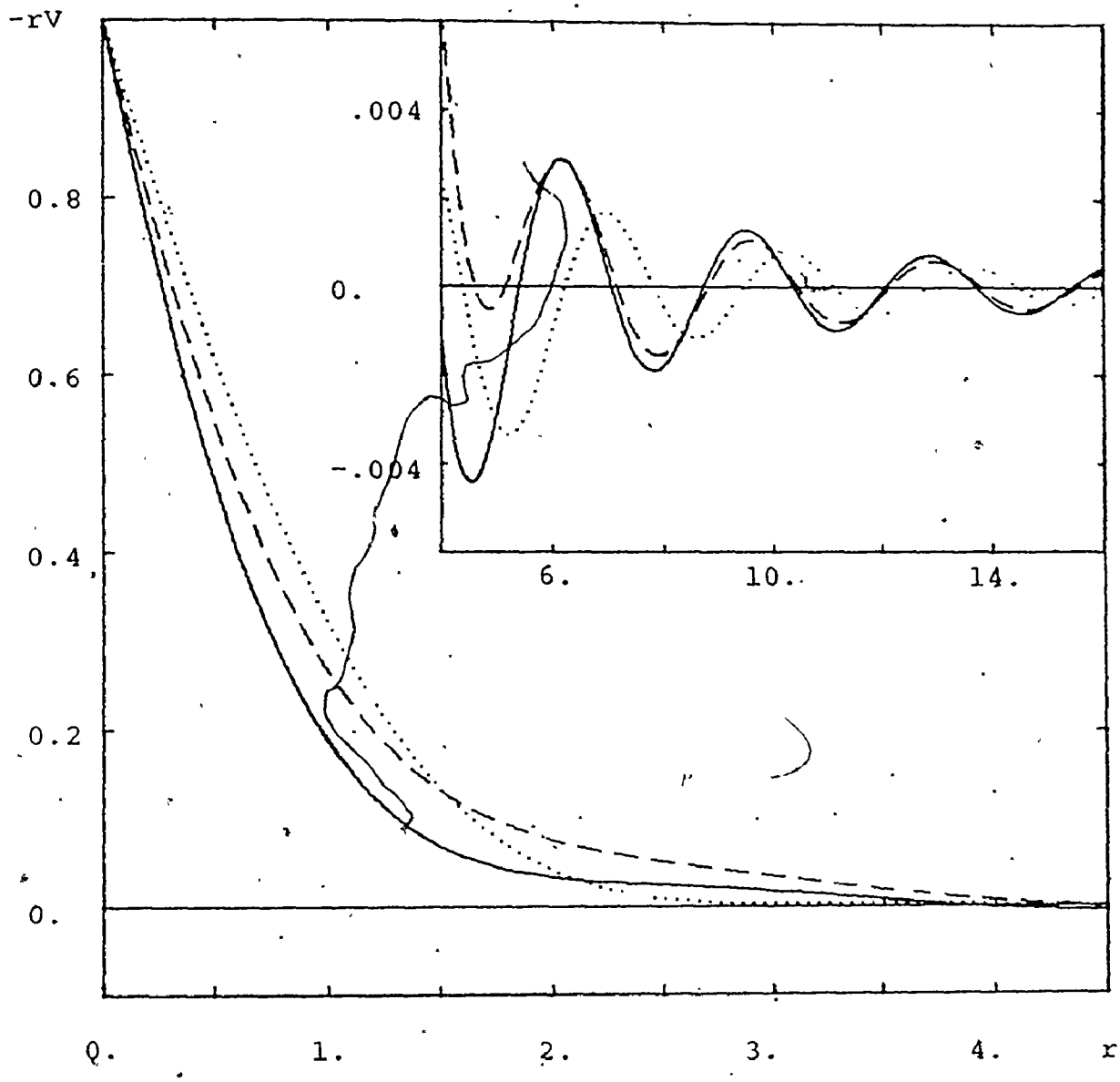

Figure 5.1: Screened electrostatic potential around a proton in aluminium. All quantities are in atomic units.

——— nonlinear theory with exchange and correlation corrections

----- nonlinear Hartree theory

..... linear theory

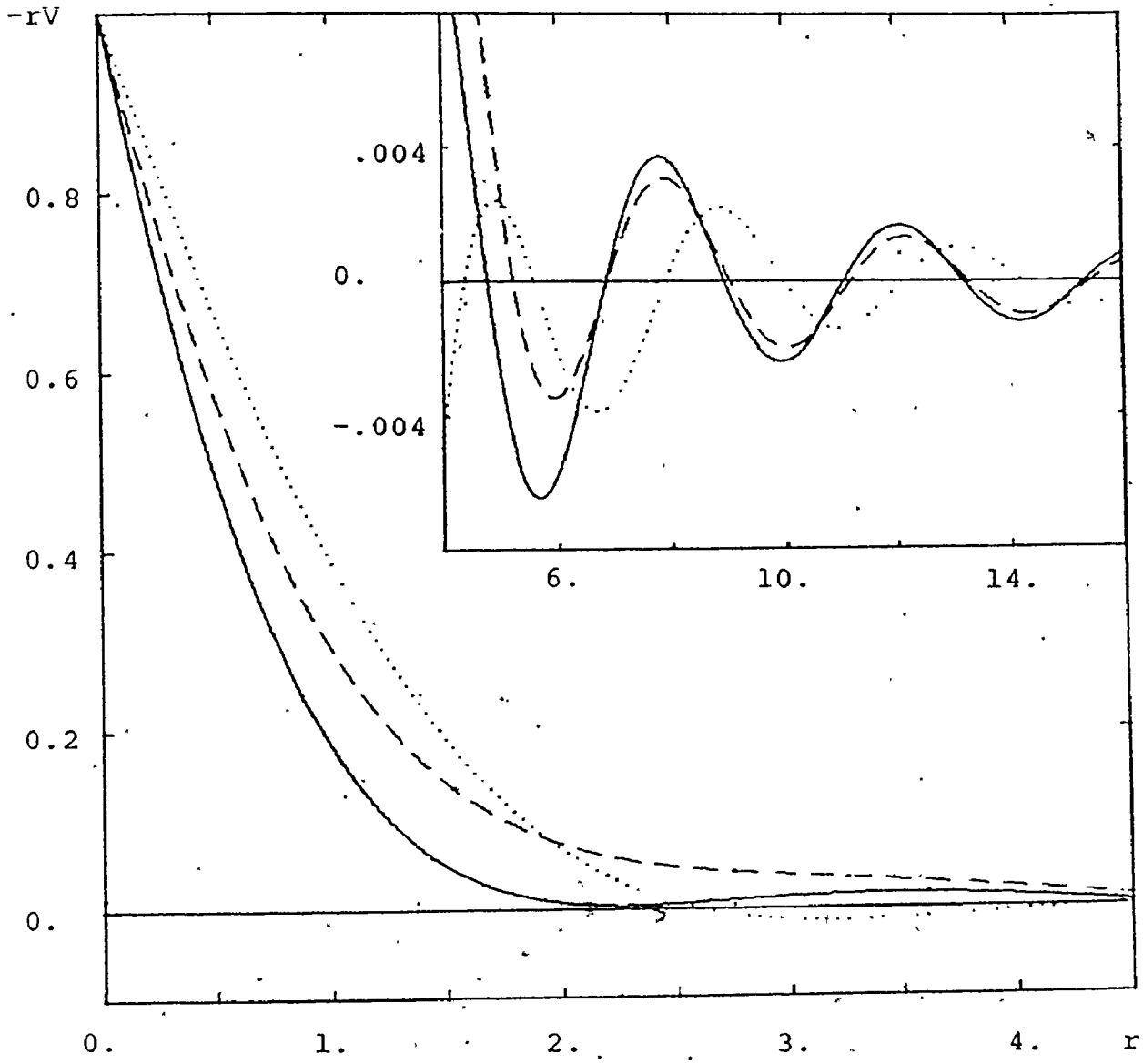

Figure 5.2: Screened electrostatic potential around a proton in magnesium. All quantities are in atomic units.

. . . nonlinear theory with exchange and correlation corrections

——— nonlinear Hartree theory

----- linear theory

required to satisfy the Friedel sum rule. Linear theory cannot produce the correct phase at large distances, as it always gives zero phase shift.

The dramatic difference in screening is most directly seen if we compare the electron densities in the screening cloud as a function of distance (Figures 5.3 and 5.4). At the proton site the nonlinear theory gives a large charge pileup: for Al about 6 times and for Mg about 10 times larger than the corresponding linear screening results. For comparison the electron density in atomic hydrogen is also presented. As one might expect it is smaller than in a metal, but of the same order of magnitude. The large charge pileup around a positive point impurity of finite mass has been described before in the case of a positron (Carbotte 1967, Sjölander and Stott 1972). The pileup is much more pronounced for a proton, which due to its large mass scatters the electrons more strongly. The charge density at the proton site is roughly four times larger than in the positron case.

5.5 Nonlinear Proton Screening Corrections to the Heat of Solution of Hydrogen

As mentioned in Section 5.2, where a linear theory of the hydrogen heat of solution was developed, the terms

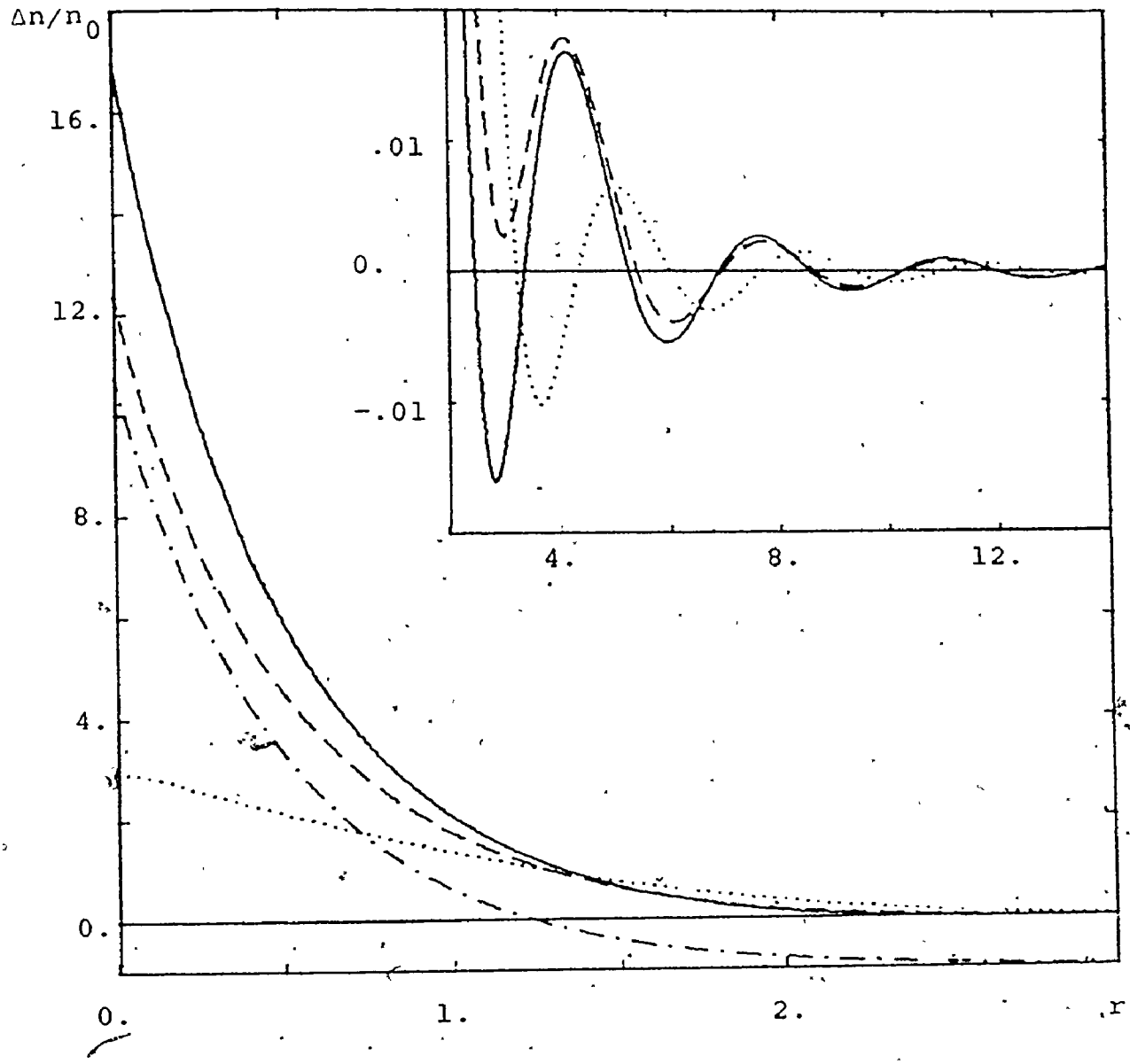

Figure 5.3: Electron density in the screening cloud $\Delta n(r) = n(r) - n_0$ around a proton in aluminium. Distance r is in atomic units.

——— nonlinear theory with exchange and correlation corrections

– – – – – nonlinear Hartree theory

. . . . . linear theory

–.–.– hydrogen atom

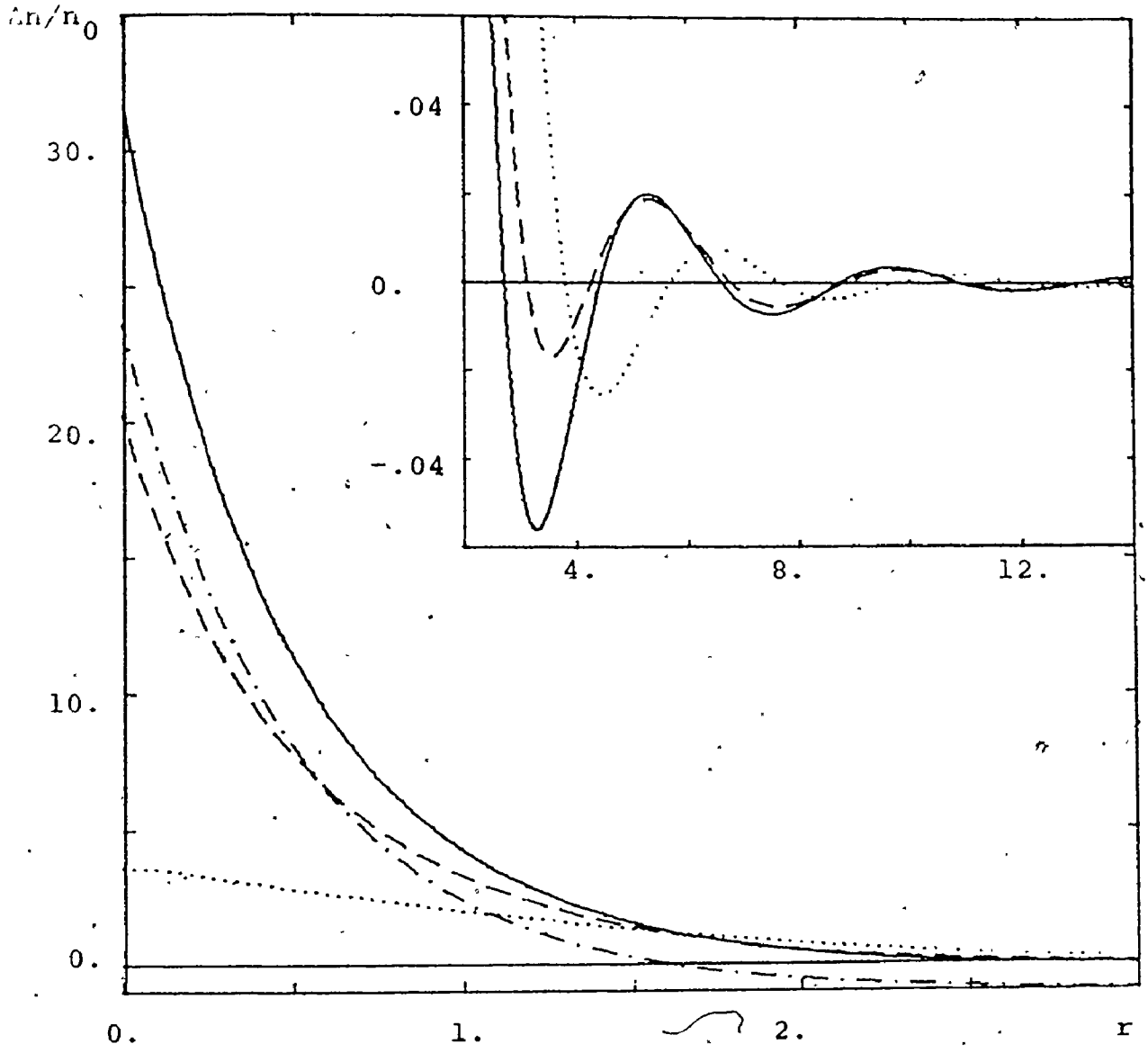

Figure 5.4: Electron density in the screening cloud $\Delta n(r) = n(r) - n_0$ around a proton in magnesium. Distance r is in atomic units.

——— nonlinear theory with exchange and correlation corrections

– – – – – nonlinear Hartree theory

. . . . . linear theory

–.–.– hydrogen atom

that linear response is not capable of describing satisfactorily depend on proton screening and are given as ΔH_2 (Eq. (5.15)). In order to introduce our nonlinear screening results into ΔH_2 we will rewrite it in a clearer form. In linear response the first term in (5.15) can be interpreted as the interaction energy between ions and the screening cloud around the proton. The second term is simply the proton correlation energy V_p so that (5.15) can be rewritten as

$$\Delta H_2 = V_p + \Delta V_p \tag{5.34}$$

with

$$\Delta V_p = \Omega_0 \sum_{q_0}' w(q) \Delta n(q) \cos \vec{q}\vec{\rho}_H \quad , \tag{5.35}$$

where the Fourier transform of the spherically symmetric electron density in the screening cloud is given by

$$\Delta n(q) = \frac{1}{\Omega_0} \int_0^\infty 4\pi r^2 \Delta n(r) \frac{\sin qr}{qr} dr \quad . \tag{5.36}$$

Formula (5.34) can be used directly to calculate ΔH_2 in nonlinear theory. When $\Delta n(q)$ is the Fourier transform of the nonlinear screening electron density, Equation (5.35) gives the first order perturbation theory correction to the proton correlation energy due to the presence of the ions.

The results of calculation for both linear and nonlinear screening are given in Table 5.5. As explained before, ΔH_1, depending only on the properties of the perfect lattice, is taken over from the linear pseudopotential theory. In calculating first order perturbation corrections to the proton correlation energy ΔV_p (Equation (5.35)), the bare ion potential form factor w(q) defined by Equation (3.4) is used, with the parameters given in Table 5.1. $\Delta n(q)$ is calculated using (5.36) in which the integral when evaluated numerically up to r = 20 gives satisfactory convergence. The values of ΔV_p differ significantly for different theories. This difference between the results of linear theory and nonlinear theories is especially large because of the difference in phase of the screened potential of the proton at large distances (see Figures 5.1 and 5.2). Proton correlation energies which enter ΔH_2, and have been calculated for different screening theories, are taken from Tables 5.2 and 5.3.

It was mentioned before that linear theory largely overestimates the heat of solution. Table 5.5 shows that nonlinear Hartree theory does not bring much improvement, which is mostly due to the still large underestimate of the proton correlation energy. In order to obtain better agreement between experimental and theoretical values, it is essential to include exchange and correlation corrections. The full theory underestimates the heat of solution by 0.2 eV

TABLE 5.5

RESULTS OF HYDROGEN HEATS OF SOLUTION CALCULATIONS AND COMPARISON WITH EXPERIMENTS

	Al	Mg
ΔH_1 (a.u.)	-0.1472	-0.1331
ΔV_p (a.u.)		
Linear Theory	0.0382	0.0003
Nonlinear (Hartree)	0.0806	0.0294
Nonlinear (exch + corr)	0.1033	0.0447
ΔH_2 (a.u.)		
Linear Theory	-0.3626	-0.3433
Nonlinear (Hartree)	-0.3708	-0.3726
Nonlinear (exch + corr)	-0.4189	-0.4469
ΔH_H (eV)		
Linear Theory	1.99	2.89
Nonlinear (Hartree)	1.76	2.03
Nonlinear (exch + corr)	0.45	-0.05
EXPERIMENTAL	0.66[a]	0.25[b]

[a] Eichenauer 1968

[b] Chapter II

for both Al and Mg. However, this discrepancy is small compared to the roughly 2 eV discrepancy which linear and nonlinear Hartree theory give.

To be able to better understand the difficulties in calculating the heat of solution of hydrogen, it should be kept in mind that it is given as a difference of energies of about 15 eV, and that its value is of the order of 0.5 eV. In view of these facts, and all the approximations that have been made, the discrepancy of 0.2 eV between experimental and theoretical results is not large and we can really regard the full theoretical calculation as successful.

CHAPTER VI

GENERAL DISCUSSION AND CONCLUSIONS

This thesis has dealt with two specific types of point defects in metals, i.e., vacancies and a hydrogen atom as an interstitial impurity. The physical quantities we have chosen to investigate are the formation energy and formation volume for vacancies and the heat of solution of hydrogen.

The problem of theoretical calculation of the properties of a vacancy was treated within the framework of local pseudopotential theory. The theories developed before (Ho 1971, Chang and Falicov 1971) were carefully and critically reexamined. Some conceptional difficulties have been resolved and the new formulated theory successfully applied to calculate formation energies and volumes of vacancies in alkalis and aluminum. An approximate scheme for treating the influence of temperature on the properties of vacancies has been proposed. When applied to aluminum it gave improved agreement with experiments.

The heat of solution of hydrogen was first calculated using local pseudopotential theory, and the results obtained were far from the experimental values. It was noted, however, that the heat of solution can be

decomposed into two parts, one due to the introduction of an electron, and the other due to the introduction of a proton in a metal. While the electronic contribution can be satisfactorily treated using pseudopotential theory, for the proton contribution it is necessary to use the more exact theory that goes beyond linear screening. The density functional formalism (Hohenberg and Kohn 1964, Kohn and Sham 1965), based on the exact numerical solution of the one particle Schroedinger equation represents a suitable framework for attacking the proton problem. However, the set of equations given by the formalism are very difficult to solve exactly. We have found a method to obtain an approximate self-consistent solution using a two parameter trial function for the effective potential. With the exchange and correlation corrections included approximately, the theory gave very good agreement between the theoretical and experimental heats of solution of hydrogen in aluminum and magnesium.

Our successful calculation of the heat of solution indicates that the density functional formalism with the existing approximations for the exchange and correlation corrections gives a satisfactory description for the electrons screening the proton. It should be possible to use our results for the screening charge density and electrostatic potential to calculate other properties of hydrogen in simple metals, such as activation energy for

diffusion, residual resistivity, Knight shift, and binding energies to different solutes (March and Rousseau 1971, Ziman 1964). The question that has still to be more carefully investigated is the possibility of one bound electron screening the proton. We believe that with further refinements and solution of some computational problems, the density functional formalism is capable of providing the answer.

In summary, the following are the main contributions of this work.

1. The solubility of hydrogen in magnesium has been measured in the temperature interval 400°C - 600°C for hydrogen pressures between 50 mmHg and 760 mmHg. The experimental results for the solubility (in units cm^3 NTP H_2/100 gr Mg) can be represented in the form:

$$S = (608 \pm 150)\left(\frac{p}{p_0}\right)^{1/2} \exp[-(5820 \pm 500)/RT] ,$$

giving the heat of solution of hydrogen in magnesium of 5820 ± 500 kcal/$\frac{1}{2}$ mole H_2 or 0.25 ± 0.02 eV/atom.

2. An improved pseudopotential theory of vacancy formation energies and volumes in alkali metals and aluminum has been formulated. The results of calculations are in good agreement with experiments.

3. The pseudopotential theory of the heat of solution of hydrogen has been developed. Poor agreement with experiments was attributed to the inadequate treatment of proton screening by linear theory.

4. The nonlinear screening theory was applied to the case of a proton and a method for an approximate self-consistent solution proposed. The results were applied to the heat of solution of hydrogen in magnesium and aluminum and satisfactory agreement with experimental values was obtained.

APPENDIX A

LATTICE STATICS OF CLOSE PACKED HEXAGONAL METALS: VACANCY IN MAGNESIUM

(Popović and Carbotte, 1974a)

Abstract

We have formulated the lattice statics method for hexagonal close packed metals and applied it to a vacancy in magnesium. Both near neighbour and asymptotic displacements have been calculated and compared. The results indicate that, as in cubic metals the elastic limit is achieved far from the defect and that the asymptotic displacements are very anisotropic.

The calculated relaxation energy indicates that in Mg, as is the case in Al, the relaxation contribution to the vacancy formation energy is small. To describe the interatomic interactions we have used two different methods: force constants deduced from the neutron scattering data and interatomic potentials calculated from Shaw's nonlocal model potential.

1. Introduction

For the calculation of atomic displacements around point defects in cubic crystals two approaches have been used, the lattice statics method (Kanzaki 1957, Flocken and Hardy 1969, Kenney et al. 1973) and the 'semidiscrete method' (Shyu et al. 1967). The first method is based on the Fourier transformation of the lattice displacements and forces acting on the atoms. In the semidiscrete method the atom displacements are calculated in a suitably chosen region (region I) and matched to the asymptotic elastic solution outside (region II). In principle this method should give a solution of any desired accuracy when region I is large enough.

However, by using the lattice statics method it has been shown (Boyer and Hardy 1971) that the elastic limit is achieved far from the defect. This makes the semidiscrete method impractical as the number of atoms that are needed in region I tends to be very large.

Therefore, in treating a vacancy in hexagonal crystals we have chosen to use the lattice statics formalism. This method has been extensively applied to cubic crystals, but not to the other structures. In section 2 of the paper we develop the lattice statics formalism for hexagonal crystals and also give formulas for the asymptotic displacements (elastic limit) and the relaxation energy of the defect. In section 3 results are presented and discussed. Conclusions are given in section 4.

Lattice Statics Method for Hexagonal Crystals

The derivation of the lattice statics method for close packed hexagonal metals follows exactly the same lines as for cubic metals (Kanzaki 1957, Flocken and Hardy 1969). However, as there are two atoms per unit cell in the close packed hexagonal case the generalization of extensively used formulas for cubic crystals is not evident. Therefore, an outline of the derivation for any crystal structure will be given and later specialised for HCP crystals.

To the second order in the displacements the energy of a crystal with the defect can be written as

$$\Phi = \Phi_0 + \frac{1}{2} \sum_{\substack{\alpha\kappa\ell \\ \beta\kappa'\ell'}} \phi_{\alpha\beta}^{\kappa\kappa'}(\vec{\ell}\vec{\ell}') u_\alpha^\kappa(\vec{\ell}) u_\beta^{\kappa'}(\vec{\ell}') - \sum_{\alpha\kappa\ell} [F_{0\alpha}^\kappa(\vec{\ell}) - \frac{1}{2} \sum_\beta f_{\alpha\beta}^\kappa(\vec{\ell}) u_\beta^\kappa(\vec{\ell})] u_\alpha^\kappa(\vec{\ell}) \quad . \qquad (1)$$

In this expression $\phi_{\alpha\beta}^{\kappa\kappa'}(\vec{\ell}\vec{\ell}')$ are interatomic force constants, $F_{0\alpha}^\kappa(\vec{\ell})$ are the forces due to the defect on the atoms in their unrelaxed configuration, $f_{\alpha\beta}^\kappa(\vec{\ell})$ are the force constants for the defect giving, to the first order, the change in the forces due to the relaxation, $\vec{\ell}$ is the position vector of the ℓ^{th} unit cell and κ is labeling atoms in the unit cell.

The energy will have a minimum when $\partial\Phi/\partial u_\alpha^\kappa(\vec{\ell}) = 0$, which gives the system of equations

$$\sum_{\beta\kappa'\ell'} \phi_{\alpha\beta}^{\kappa\kappa'}(\vec{\ell}\vec{\ell}') u_\beta^{\kappa'}(\vec{\ell}') = F_\alpha^\kappa(\vec{\ell}) \quad , \qquad (2)$$

where we have introduced the forces in the displaced positions

$$F_\alpha^\kappa(\vec{\ell}) = F_{0\alpha}^\kappa(\vec{\ell}) - \sum_\beta f_{\alpha\beta}^\kappa(\vec{\ell}) u_\beta^\kappa(\vec{\ell}) \quad . \tag{3}$$

Using (1), (2) and (3) for the relaxation energy (part of the energy dependent on the displacements) one obtains

$$E_R = -\frac{1}{2} \sum_{\alpha\kappa\ell} F_{0\alpha}^\kappa(\vec{\ell}) u_\alpha^\kappa(\vec{\ell}) \quad . \tag{4}$$

We now define Fourier transforms of the displacements and forces as

$$u_\beta^{\kappa'}(\vec{q}) = \sum_{\ell'} u_\beta^{\kappa'}(\vec{\ell}') e^{-i\vec{q}(\vec{\ell}'+\vec{\rho}_{\kappa'})} \quad , \tag{5}$$

$$F_\alpha^\kappa(\vec{q}) = \sum_\ell F_\alpha^\kappa(\vec{\ell}) e^{-i\vec{q}(\vec{\ell}+\vec{\rho}_\kappa)} \quad , \tag{6}$$

where $\vec{\rho}_\kappa$ is the position vector of atom κ in the unit cell. After substituting (2) in (6) and performing some simple algebraic manipulations, one obtains

$$F_\alpha^\kappa(\vec{q}) = \sum_{\beta\kappa'} D_{\alpha\beta}^{\kappa\kappa'}(\vec{q}) u_\beta^{\kappa'}(\vec{q}) \quad , \tag{7}$$

where the dynamical matrix

$$D_{\alpha\beta}^{\kappa\kappa'}(\vec{q}) = \sum_{\ell'} e^{-i\vec{q}(\vec{\ell}+\vec{\rho}_\kappa)} \phi_{\alpha\beta}^{\kappa\kappa'}(\vec{\ell}\vec{\ell}') e^{i\vec{q}(\vec{\ell}'+\vec{\rho}_{\kappa'})} \tag{8}$$

has been introduced. This definition of the dynamical matrix is the same as one used by De Wames et al. (1965) for HCP crystals.

By inverting (7) we obtain the Fourier transform of the displacements as

$$u_\alpha^\kappa(\vec{q}) = \sum_{\beta\kappa'} [D_{\alpha\beta}^{\kappa\kappa'}(\vec{q})]^{-1} F_\beta^{\kappa'}(\vec{q}) \quad . \tag{9}$$

Once we know $u_\alpha^\kappa(\vec{q})$, actual displacements can be calculated with the formula,

$$u_\alpha^\kappa(\vec{\ell}) = \frac{1}{N} \sum_q u_\alpha^\kappa(\vec{q}) e^{i\vec{q}(\vec{\ell}+\vec{\rho}_\kappa)} \quad . \tag{10}$$

However, to compute $u_\alpha^\kappa(\vec{q})$ using (8) we must know $F_\alpha^\kappa(\vec{q})$, i.e., the forces $F_\alpha^\kappa(\vec{\ell})$ acting on the atoms. But according to (3) these forces depend on the displacements $u_\alpha^\kappa(\vec{\ell})$. To solve the problem consistently we note that using (6) and (9), equation (10) can be transformed to

$$u_\alpha^\kappa(\vec{\ell}) = \sum_{\beta\kappa'\ell'} G_{\alpha\beta}^{\kappa\kappa'}(\vec{\ell}\vec{\ell}') F_\beta^{\kappa'}(\vec{\ell}') \quad , \tag{11}$$

where

$$G_{\alpha\beta}^{\kappa\kappa'}(\vec{\ell}\vec{\ell}') = \frac{1}{N} \sum_q [D_{\alpha\beta}^{\kappa\kappa'}]^{-1} e^{i\vec{q}(\vec{\ell}+\vec{\rho}_\kappa-\vec{\ell}'-\vec{\rho}_{\kappa'})} \tag{12}$$

is the static lattice Green's function (Flinn and Maradudin 1962, Bullough and Tewary 1972). As the interaction forces fall , with

distance, only those forces acting on the first few shells (say 5 to 10) can be regarded as different from zero. Then (3) and (11) give a finite system of linear equations for the displacements $u_\alpha^\kappa(\vec{\ell})$ of the atoms in those shells. After this system is solved, the forces in the displaced positions are found using (3) and the displacement of any atom can be calculated using (6), (9) and (10).

Up to this point our derivation was perfectly general for any type of crystal structure. For practical calculations exploitation of crystal symmetry gives great advantages both from the point of view of computer storage and computation time. For HCP crystals, the dynamical matrix, as defined by (8), is complex and can be represented as the supermatrix (De Wames et al. 1965)

$$\mathcal{D}(\vec{q}) = \begin{bmatrix} D^{11}(\vec{q}) & D^{12}(\vec{q}) \\ D^{12}(\vec{q})^* & D^{11}(\vec{q}) \end{bmatrix}, \tag{13}$$

where $D^{11}(\vec{q})$ is real and $D^{12}(\vec{q})$ is a complex 3×3 matrix. For practical calculations, it is much more convenient to work with real matrices. This can be accomplished by performing the unitary transformation of the equation (9) with the matrix

$$v = \frac{1}{\sqrt{2}} \begin{bmatrix} I & iI \\ -I & iI \end{bmatrix}, \tag{14}$$

where I is the 3×3 identity matrix. In doing this, (9) becomes (written in matrix form)

$$v^{+}u = (v^{+}\mathcal{D}v)^{-1}\, v^{+}\mathcal{F} \qquad (15)$$

and involves inversion of the real matrix

$$v^{+}\mathcal{D}v = \begin{bmatrix} D^{11} - \mathrm{Re}D^{12} & -\mathrm{Im}D^{12} \\ -\mathrm{Im}D^{12} & D^{11} + \mathrm{Re}D^{12} \end{bmatrix} . \qquad (16)$$

The derivation of the asymptotic limit from the lattice statics has been given by Flocken and Hardy (1970) for cubic crystals. Using essentially the same method we have calculated the two first terms in the asymptotic expansion of the displacements around a vacancy in HCP crystals. With the aid of the relations

$$\int_0^\infty x \sin(tx)dx = -\pi \frac{\partial}{\partial t}\delta(t) \quad ,$$

$$\int_0^\infty x^2 \cos(tx)dx = -\pi \frac{\partial^2}{\partial t^2}\delta(t) \quad ,$$

one easily obtains:

$$|\vec{\ell}+\vec{\rho}_\kappa|^2\, u_\alpha^\kappa(\ell\to\infty) = -\frac{\Omega_0}{8\pi^2}\int_0^{2\pi} d\phi \left\{\frac{\partial}{\partial(\cos\theta)}\, \mathrm{Im}[q u_\alpha^\kappa(q\to 0)]\right\}_{\theta=\pi/2}$$

$$- \frac{1}{|\vec{\ell}+\vec{\rho}_\kappa|}\frac{\Omega_0}{8\pi^2}\int_0^{2\pi} d\phi \left\{\frac{\partial^2}{\partial(\cos\theta)^2}\right.$$

$$\left. \times\, \mathrm{Re}[u_\alpha^\kappa(q\to 0)]\right\}_{\theta=\pi/2} + \ldots \quad , \qquad (17)$$

where the polar axis of the coordinate system defining the angles θ and ϕ, has the direction of the vector $\vec{\ell}+\vec{\rho}_\kappa$ and Ω_0 is the unit cell volume.

There is an important difference in the asymptotic expansions for the displacements around substitutional impurities in cubic and HCP crystals which is also generally valid for Bravais and non-Bravais crystals. It is easy to show that for cubic crystals the expansion has the form $\ell^2 u_{cubic} = A + B/\ell^2 + \ldots$. According to (17) for HCP crystals, $\ell^2 u_{HCP} = A' + B'/\ell + \ldots$, the second term falls off slower than in cubic crystals. Consequently for similar interatomic interactions the asymptotic limit in HCP crystals will be achieved at larger distances than in cubic crystals. The influence of the second term in the expansion (17) will be illustrated in the following section.

The difference in the asymptotic limit of lattice statics for Bravais and non-Bravais lattices is also reflected in the nature of the singularity at $q = 0$ of the static Green's function (12). For a Bravais lattice all three acoustic branches of the dispersion curves contribute to the singularity, while in a non-Bravais lattice optical modes have a non-singular contribution. Consequently the $q = 0$ contribution becomes dominant in the former case for smaller ℓ than in the latter case where the non-singular part due to the optical modes varies slowly with q**.

** We thank the referee for these clarifying remarks.

3. Results of Calculation and Discussion

The calculations were performed for the two different sets of force constants given in Table 1. The first set, derived from neutron scattering data is due to Pynn and Squires (1972). The second set is based on the full nonlocal pseudopotential calculation of interatomic interactions in Mg by Shaw and Pynn (1969). Interactions between atoms are in both cases assumed to be well described by central forces, so that for any pair of atoms there are only two independent force constants, radial and tangential (or bond stretching and bond bending, as they are sometimes called). Forces due to a vacancy can be obtained from force constants using the prescription proposed by Flocken and Hardy (1969).

The coordinate system that we used is the same as defined by De Wames et al. (1965), with the vacancy at the origin. To label different atoms with three integers, the distance in the x direction is measured in units of $a\sqrt{3}/6$, in the y direction in units of a/2 and in the z direction in units of c/2. For example, the label 1,1,1 denotes the atom with coordinates $(a\sqrt{3}/6, a/2, c/2)$. This labeling of atoms and directions will be used throughout the paper.

The results of our calculations of forces in the displaced positions as well as the first eight neighbours displacements are given in Tables 2 and 3. The forces are radial and the components of the displacements are given in polar coordinates.

Table 1

Force Constants used in the Calculations

Assumed Value of c/a = 1.622

Distance/a	Neutron Data Force Constants (dyn/cm)		Pseudopotential Data Force Constants (dyn/cm)	
	radial	tangential	radial	tangential
.996	10483	-309	13742	-429
1.000	10099	-292	13138	-378
1.411	-222	-246	-701	5
1.622	305	-490	320	1
1.730	748	13	153	17
1.732	529	91	149	17
1.906	49	157	-141	15
.000	-401	42	-203	5

Table 2

Forces and Displacements around a Vacancy in Mg based on the Force Constants Deduced from Neutron Scattering Data. For an Explanation of the Labeling Used for the Neighbouring Atoms, see Text.

Neighbour	distance/a	force (units dyn/á)		displacements		
		undisplaced	displaced	u_r/a	u_θ/a	u_ϕ/a
3, 1, 0	1.000	-292.	-337.4	-0.00449	0.0	0.00056
6, 0, 0	1.732	157.6	158.8	0.00217	0.0	0.0
3, 3, 0	1.732	157.6	159.7	0.00397	0.0	0.0
6, 2, 0	2.000	84.0	83.5	0.00125	0.0	0.00042
1, 1, 1	0.996	-307.6	-384.0	-0.00729	0.00362	0.0
4, 0, 1	1.411	-347.1	-345.2	-0.00884	-0.00197	0.0
4, 2, 1	1.730	22.5	22.4	-0.00010	-0.00012	0.00038
0, 0, 2	1.622	-794.8	-802.5	-0.02529	0.0	0.0
3, 1, 2	1.906	299.2	299.4	0.00577	0.00018	0.00035

Table 3

Forces and Displacements around a Vacancy in Mg based on the Force Constants Calculated from Shaw's Nonlocal Pseudopotential Theory. For an Explanation of Labeling used for the Neighbouring Atoms, see Text.

Neighbour	distance/a	force (units dyn/a)		displacements		
		undisplaced	displaced	u_r/a	u_θ/a	u_ϕ/a
3, 1, 0	1.000	-378.0	-494.5	-0.00886	0.0	-0.00107
6, 0, 0	1.732	29.4	29.3	-0.00127	0.0	0.0
3, 3, 0	1.732	29.4	29.1	-0.00254	0.0	0.0
6, 2, 0	2.000	10.0	10.6	-0.00292	0.0	0.00019
1, 1, 1	0.996	-427.1	-573.3	-0.01064	0.00043	0.0
4, 0, 1	1.411	7.1	6.8	-0.00031	0.00026	0.0
4, 2, 1	1.730	29.4	29.1	-0.00210	-0.00021	-0.00016
0, 0, 2	1.622	1.6	0.6	-0.00328	0.0	0.0
3, 1, 2	1.906	28.6	28.9	-0.00227	0.00015	0.00058

For the two sets of force constants, the displacements differ significantly. The relaxation energy (4) is - 0.033 eV for neutron scattering data and - 0.015 for Shaw's pseudopotential. Although these two numbers are quite different, they both indicate that in Mg as in Al (Popović et al. 1974) the relaxation energy does not make a significant contribution to the vacancy formation energy.

We have also calculated asymptotic displacements and compared them with the results of the exact calculation. The results are given in Tables 4, 5 and 6. The numbers n_x, n_y and n_z quoted in the tables denote the orders of the Gauss' integration formulas used for the integration in the q_x, q_y and q_z directions, respectively. The integration interval in the q_x direction is $[0, 2\pi/a\sqrt{3}]$, in the q_y direction is $[-q_x/\sqrt{3}, + q_x/\sqrt{3}]$ and in the q_z direction is $[0, 2\pi/c]$ which was transformed to the interval $[- \pi/c, \pi/c]$ by using the periodic properties of Fourier transforms. To integrate over the angle ϕ in (17) an integration formula of 24th order was used and the derivatives with respect to $\cos\theta$ were calculated numerically.

For the neutron scattering force constants the cancelation of positive and negative terms is large so that the first term in (17) is relatively small. To achieve agreement between the asymptotic and exact calculations it was necessary to include two terms of the asymptotic expansion (17). When the second term does not contribute to the displacements, the corresponding column in the tables is omitted.

Table 4

Comparison of Exact and Asymptotic Displacements for the (3, 1, 0) Direction

$n_x = 20$, $n_y = 22$, $n_z = 20$. $u_\theta \equiv 0$

atom	distance/a	Neutron Data			Pseudopotential Data		
		$\ell^2 u_r/a^3$	$\ell^2 u_\phi/a^3$		$\ell^2 u_r/a^3$	$\ell^2 u_\phi/a^3$	
		exact	exact	asymptotic	exact	exact	asymptotic
, 1, 0	1.0	-0.00449	0.00056	-0.00502	-0.00886	-0.00106	0.00865
, 3, 0	3.0	0.00480	0.00224	-0.00167	-0.01091	-0.00036	0.00288
5, 5, 0	5.0	0.00170	0.00088	-0.00100	-0.00930	0.00040	0.00173
1, 7, 0	7.0	0.00111	0.00006	-0.00072	-0.00854	0.00070	0.00124
7, 9, 0	9.0	0.00093	-0.00019	-0.00055	-0.00813	0.00073	0.00096
3, 11, 0	11.0	0.00084	-0.00026	-0.00046	-0.00788	0.00068	0.00079
9, 13, 0	13.0	0.00080	-0.00027	-0.00039	-0.00771	0.00061	0.00067
	∞	0.00066		0.00000	-0.00724		0.00000

Table 5

Comparison of Exact and Asymptotic Displacements for the (1, 1, 1) Direction

$n_x = 16,\ n_y = 18,\ n_z = 24.\quad u_\phi \equiv 0$

atom	distance/a	Neutron Data				Pseudopotential Data			
		$\ell^2 u_r/a^3$		$\ell^2 u_\theta/a^3$		$\ell^2 u_r/a^3$		$\ell^2 u_\theta/a^3$	
		exact	asymp	exact	asymp	exact	asymp	exact	asymp
1, 1, 1	.996	-.00723	.00949	.00359	.00097	-.01055	-.01028	.00043	-.00073
7, 7, 7	6.969	.00160	.00111	.00013	.00028	-.00616	-.00626	.00031	.00034
13, 13, 13	12.942	.00055	.00047	.00017	.00023	-.00593	-.00595	.00042	.00042
19, 19, 19	18.915	.00026	.00023	.00018	.00021	-.00582	-.00584	.00046	.00045
	∞		-.00029		.00017		-.00559		.00051

Table 6

Comparison of Exact and Asymptotic Displacements in the (0, 0, 2) Direction (c-axes)

$n_x = 14$, $n_y = 16$, $n_z = 48$ for Neutron Data and

$n_x = 14$, $n_y = 16$, $n_z = 24$ for Pseudopotential Data

atom	distance/a	Neutron Data $\ell^2 u_r/a^3$	Pseudopotential Data $\ell^2 u_r/a^3$
0, 4	3.442	-0.01361	-0.0102
0, 8	6.488	-0.00336	-0.0118
0, 0, 12	9.732	-0.00184	-0.0121
0, 16	12.976	-0.00138	-0.0122
0, 20	16.220	-0.00119	-0.0122
0, 24	19.464	-0.00109	-
0, 28	22.708	-0.00102	-
0, 32	25.952	-0.00098	-
0, 36	29.196	-0.00095	-
0, 40	32.440	-0.00092	-
0, 44	35.684	-0.00089	-
	∞	-0.00088	-0.0123

As noted by Boyer and Hardy (1971) integration over the BZ using Gauss integration formulas breaks down when the distance of the atom becomes so large as to produce a number of nodes in the integration interval approximately equal to the order of the integration formula. Our results are given only within a distance before the breakdown occurs. To check the agreement between asymptotic and directly calculated displacements using a reasonable amount of computation time, the atoms in the c-direction are specially convenient. For those atoms great accuracy in integration can be achieved by taking the order of integration formula n_z large while keeping n_x and n_y relatively small. The results are given in Table 6 with excellent agreement between directly and asymptotically calculated displacements.

The asymptotic limit for the pseudopotential data is achieved much closer to the defect than for the neutron scattering data. There are two reasons for this. First, as already mentioned, neutron scattering data give small asymptotic displacements indicating large cancelation of the first term in (17). Second, pseudopotential data can actually be regarded as a nearest neighbour model because the forces due to the vacancy are significant for nearest neighbours only.

Finally, in Table 7 the angular dependence of the asymptotic displacements is given, with the c-axis taken as the polar axis. The asymptotic displacements do not depend on angle ϕ, and the component $u_\phi \equiv 0$. That is a direct consequence of elastic isotropy of hexagonal crystals in the basal plane and

Table 7

Angular Dependence of Asymptotic Displacements. $u_\phi \equiv 0$

θ (in degrees)	Neutron Data		Pseudopotential Data	
	$\ell^2 u_r/a^3$	$\ell^2 u_\theta/a^3$	$\ell^2 u_r/a^3$	$\ell^2 u_\theta/a^3$
0	-0.00088	0.00000	-0.0123	0.0000
10	-0.00081	0.00007	-0.0111	0.0006
20	-0.00064	0.00013	-0.0086	0.0008
30	-0.00041	0.00016	-0.0064	0.0007
40	-0.00018	0.00017	-0.0051	0.0004
50	0.00005	0.00017	-0.0046	0.0000
60	0.00027	0.00016	-0.0048	-0.0003
70	0.00046	0.00012	-0.0057	-0.0004
80	0.00061	0.00007	-0.0068	-0.0003
90	0.00066	0.00000	-0.0072	0.0000

hexagonal symmetry of the forces due to the presence of a vacancy. As seen from the table the displacements show considerable anisotropy.

4. Conclusion

We have developed the lattice statics formalism for close packed hexagonal metals and applied it to a vacancy in magnesium. The two different sets of force constants used in the calculations (based on neutron scattering data and nonlocal pseudopotential theory) differ significantly. However, both sets of data indicate that relaxations around vacancies in Mg are small (around 1% for nearest neighbours). Therefore, the lattice statics formalism, which does not take into account nonlinear effects, is adequate in describing atom relaxations around vacancies in magnesium. Small relaxation energies in both cases indicate that the vacancy formation energy is not very much influenced by atomic relaxations. Therefore, the assumption of an unrelaxed lattice might be a good starting point for the calculations of other physical pro erties connected with vacancies, as is for example, the activation energy for self diffusion via the vacancy mechanism (Du Charme and Weaver 1972).

APPENDIX B

THE INFLUENCE OF LATTICE STRAIN ON THE RESIDUAL RESISTIVITY OF DILUTE ALKALI ALLOYS

(Popović, Carbotte, and Piercy 1973)

Abstract

The effect of lattice distortion on the residual resistivity of dilute alkali alloys has been calculated using the lattice statics method due to Kanzaki and the empty core Ashcroft model pseudopotential. The dielectric function due to Singwi et al. was used for calculating the ion-ion and ion-electron interaction potentials. The correction for lattice distortion was found to be 5 - 30%, which confirms the estimate given by Ziman. The overall agreement with experiment is of the same order as the phase shift calculation without lattice distortion.

1. Introduction

The electrical resistivity due to simple defects (vacancies, substitutional impurities) has been calculated for a number of metals using either phase shifts or pseudopotential form factors to describe the effective potential of a point defect (Harrison 1966, Dickey et al. 1967, Fukai 1969, Meyer et al. 1971). However, it was only very recently that the influence of the lattice strain was included in the calculation of the vacancy resistivity in Na, K and Al (Benedeck and Baratoff 1971). Following closely the work on vacancies, we have calculated the residual resistivity of substitutional alkali impurities in alkali metals, using a pseudopotential formalism and including the influence of lattice relaxation within the formalism of lattice statics.

2. Residual Resistivity

Within the framework of a weak pseudopotential approximation the distortion of the lattice enters the resistivity calculation through the structure factor

$$S(\underset{\sim}{q}) = \sum_{\underset{\sim}{\ell}} e^{-i\underset{\sim}{q}(\underset{\sim}{\ell}+\underset{\sim}{u}^{\ell})} , \qquad (1)$$

where $\underset{\sim}{\ell}$ is the equilibrium ion position in the perfect lattice and $\underset{\sim}{u}^{\ell}$ is the displacement due to the presence of the defect.

As the Fermi surface of the alkali metals lies completely in the first Brillouin zone and is nearly spherical, electron states are well represented by plane waves. For calculating electrical resistivity it is necessary to know matrix elements for the transition between states $\underset{\sim}{k}$ and $\underset{\sim}{k}'$ when both are lying on the Fermi surface. It is straightforward to show that (Fukai 1969)

$$\langle \underset{\sim}{k} | V_{scatt} | \underset{\sim}{k}' \rangle = \frac{1}{N} \{ (S(\underset{\sim}{q})-1) w_H(q) + w_I(q) \} \qquad (2)$$

where $\underset{\sim}{q} = \underset{\sim}{k}' - \underset{\sim}{k}$ and $w_H(q)$ and $w_I(q)$ are pseudopotential form factors of host and impurity atoms. We can write the structure factor as the sum of the structure factor of the perfect lattice $S_0(\underset{\sim}{q})$ and the change due to the presence of the defect

$$S(\underset{\sim}{q}) = S_0(\underset{\sim}{q}) + \Delta S(\underset{\sim}{q}) \quad .$$

$S_0(\underset{\sim}{q})$ is different from zero only for $\underset{\sim}{q}$ equal to the reciprocal lattice vector $\underset{\sim}{G}$. Since two wavevectors on the Fermi surface of alkali metals always have $\underset{\sim}{q}$ smaller than the smallest $\underset{\sim}{G}$, we can write equation (2) as

$$\langle \underset{\sim}{k} | V_{scatt} | \underset{\sim}{k}' \rangle = \frac{1}{N} \{ [\Delta S(\underset{\sim}{q})-1] w_H(q) + w_I(q) \} \qquad (3)$$

where

$$\Delta S(\underset{\sim}{q}) = \sum_{\underset{\sim}{\ell}} e^{-i\underset{\sim}{q}\underset{\sim}{\ell}} (e^{-i\underset{\sim}{q}\underset{\sim}{u}^{\ell}} - 1)$$

$$\approx -i\underset{\sim}{q} \sum_{\ell} \underset{\sim}{u}^{\ell} e^{-i\underset{\sim}{q}\underset{\sim}{\ell}} = S_1(\underset{\sim}{q}) \quad . \qquad (4)$$

For vacancies Benedeck and Baratoff (1971) found that higher order terms in the expansion (4) can be neglected. Since a substitutional impurity will produce relaxation of the same order as a vacancy, we expect this approximation to be sufficiently accurate for dilute alkali alloys.

Once we have the scattering matrix elements, the impurity resistivity can easily be calculated using the standard formula

$$\rho_I = \frac{3m^{*2}\Omega_0 n_I}{16\hbar^3 e^2 k_F^2} \int_{|\zeta|<2} |\langle \mathbf{k}_F+\mathbf{q}|V_{scatt}|\mathbf{k}_F\rangle|^2 \frac{\zeta d^3\zeta}{\epsilon(q)^2} \quad , \qquad (5)$$

where n_I is impurity concentration, m* effective mass, Ω_0 atomic volume and $\zeta = q/k_F$. Strictly speaking, equation (5) is exact only for isotropic scattering. Due to the presence of $\Delta S(q)$ in (3) scattering from the relaxed defect will not be isotropic. However, Green and Kohn (1965) have shown that (5) can also be applied with reasonable accuracy for moderately anisotropic scattering. So, once we know the pseudopotential form factors, to include relaxation we have only to calculate the change of the structure factor (4).

3. Structure Factor

Three approaches have been used to calculate the effect of lattice distortion on various properties of point defects: the lattice statics method (Kanzaki 1957), the "semidiscrete" method (Shyu et al. 1967) and the continuum approximation (Beal-Monod and Kohn 1968). Flocken and Hardy (1969), who used the

first method extensively have undoubtedly shown the inadequacy of the continuum approximation. It is not valid simply because the elastic limit is only achieved very far from the defect (Boyer and Hardy 1971). In the discrete method the atom displacements are calculated in a suitable chosen region (region I) and matched to the asymptotic elastic solution outside (region II). In principle this method should give a solution of any desired accuracy when region I is large enough. When applied without reducing the number of variables by symmetry, it has the advantage of being applicable to both simple and more complex defects (Lidiard 1972). However, the lattice statics method has a special advantage for calculation of the electrical resistivity caused by simple defects, as it directly gives the change of structure factor (4), which is all that we need. Symmetry properties, which substantially reduce both computation time and memory requirements, are also easily taken into account.

According to the fundamental equations of lattice statics (Kanzaki 1957, Flocken and Hardy 1969) the Fourier transforms of the atomic displacements and of the force array due to the defect

$$\underset{\sim}{u}^{q} = \sum_{\underset{\sim}{\ell}} \underset{\sim}{u}^{\ell} \, e^{-i\underset{\sim}{q}\underset{\sim}{\ell}} \quad , \tag{6}$$

$$\underset{\sim}{F}^{q} = \sum_{\underset{\sim}{\ell}} \underset{\sim}{F}^{\ell} \, e^{-i\underset{\sim}{q}\underset{\sim}{\ell}} \quad , \tag{7}$$

are connected by the simple relation

$$\underset{\sim}{u}^{q} = [\underset{\sim}{D}^{q}]^{-1} \, \underset{\sim}{F}^{q} \quad , \tag{8}$$

where $D^{q}_{\tilde{}}$ is the dynamical matrix

$$D^{q}_{\alpha\beta} = \sum_{\ell} \phi^{\ell}_{\alpha\beta} \; e^{-iq\ell} \quad . \tag{9}$$

Comparing (4) and (6) we see that the structure factor $S_1(q)$ is

$$S_1(q) = -iqu^{q} \quad . \tag{10}$$

Thus, the only quantity needed is $u^{q}_{\tilde{}}$ and it is simply connected to $F^{q}_{\tilde{}}$.

To compute $F^{q}_{\tilde{}}$ we have to know the forces $F^{\ell}_{\tilde{}}$ acting on the atoms. However, these forces will also depend on the displacements $u^{\ell}_{\tilde{}}$, as the forces entering (7) are evaluated at the displaced positions. If we expand the force around the non-relaxed position as

$$F^{\ell}_{\alpha} = F^{\ell}_{0\alpha} + \sum_{\beta} f^{\ell}_{\alpha\beta} \; u^{\ell}_{\beta} \tag{11}$$

we can take into account, at least to the first order, the change in forces due to the displacements (Flocken and Hardy 1969).

Equations (6), (7) and (8) can be transformed to give

$$u^{\ell}_{\alpha} = \sum_{\ell'\beta} G^{\ell\ell'}_{\alpha\beta} \; F^{\ell'}_{\beta} \tag{12}$$

where

$$G^{\ell\ell'}_{\alpha\beta} = \frac{1}{N} \sum_{q} (D^{q}_{\tilde{}})^{-1}_{\alpha\beta} \; e^{iq(\ell-\ell')} \tag{13}$$

is the static lattice Green's function (Flinn and Maradudin 1962).

As interionic forces fall off rapidly with distance, only those acting on the first few shells (say 5-10) can be regarded as different from zero and then (11) and (12) give a finite system of linear equations for the displacements u_α^ℓ. After this system is solved, the forces in the displaced positions are found using (11).

4. Ionic Interactions

Pseudopotential theory was used to calculate both force constants entering the dynamical matrix (9) and the forces on the atoms due to the defect ($F_{0\alpha}^{\ell}$ and $f_{\alpha\beta}^{\ell}$ in (11)). The host-host interaction potential is given by (Shyu and Gaspari 1968)

$$V(r) = \frac{Z^2e^2}{r} - \frac{2Z^2e^2}{\pi}\int_0^\infty G(q)\,\frac{\sin qr}{qr}\,dq \qquad (14)$$

with

$$G(q) = \left(\frac{4\pi Ze^2}{\Omega_0 q^2}\right)^{-2}\frac{w_H(q)^2}{1-f(q)}\left(1 - \frac{1}{\varepsilon(q)}\right) \qquad (15)$$

where $w_H(q)$ is the bare ion pseudopotential form factor of the host lattice, for which an Ashcroft analytic form was assumed

$$w_H(q) = -\frac{4\pi Ze^2}{\Omega_0 q^2}\cos qr_c \quad , \qquad (16)$$

and $\varepsilon(q)$ is the electron dielectric function:

$$\varepsilon(q) = 1 + (1-f(q))\,\frac{4\pi e^2}{\Omega_0 q^2}\left(\frac{2}{3}\cdot\frac{\hbar^2k_F^2}{2m^*}\right)^{-1} \times \left[\frac{1}{2} + \frac{4k_F^2 - q^2}{8k_Fq}\,\ell n\left|\frac{2k_F+q}{2k_F-q}\right|\right] \qquad (17)$$

The analytic form for the function f(q)

$$f(q) = A[1 - e^{-B(q/k_F)^2}] \quad , \tag{18}$$

where A and B are parameters dependent on the electron density, was taken from Singwi et al. (1970).

The additional interaction potential $V_I(r)$ due to the presence of the defect can easily be obtained from the standard formula for the total energy of the crystal (Harrison 1966, Shyu and Gaspari (1968), by replacing the square of the ion potential Fourier transform $|S(q)w_H(q)|^2$ by the square of the Fourier transform of the electron potential when the impurity is present:

$$W(\underset{\sim}{r}) = \sum_{\underset{\sim}{\ell}} w_H(\underset{\sim}{r}-\underset{\sim}{r_\ell}) + \Delta w(\underset{\sim}{r}) \quad , \tag{19}$$

with $\Delta w(r) = w_I(r) - w_H(r)$. The result is

$$V_I(r) = -\frac{2Z^2e^2}{\pi} \int_0^\infty G_1(q) \frac{\sin qr}{qr} dq \tag{20}$$

where $G_1(q)$ has the same form (15) as G(q), with $w_H(q)^2$ replaced by $w_H(q)\Delta w(q)$.

For the ions interacting through the central interaction potential, there are only two independent force constants, the radial K_r and tangential K_t given by

$$K_t = \frac{1}{r}\frac{dV}{dr} \quad , \quad K_r = \frac{d^2V}{dr^2} \quad , \tag{21}$$

for host-host interaction and by

$$K_{It} = \frac{1}{r}\frac{dV_I}{dr} \quad , \quad K_{Ir} = \frac{d^2V_I}{dr^2} \quad , \qquad (22)$$

for host-impurity interaction. These are further simply connected with $\phi^{\ell}_{\alpha\beta}$ in (9) and $F^{\ell}_{0\alpha}$ and $f^{\ell}_{\alpha\beta}$ in (11).

5. Results of Calculation and Discussion

The data used in the calculation for the ion core radius r_c, the effective mass m*, the lattice parameters, and the values of A and B in (18) were all taken from Price et al. (1970). The forces due to the defect and the force constants in the dynamical matrix were calculated using (14), (20-22). For both host-host and host-impurity interactions, it was assumed that the forces are negligible after the fifth shell. Since for lithium it was established that the forces are of larger range (Flocken and Hardy 1969), for this element calculations were done with both five and eight shells. It was found that the five shell results did not differ by more than 2 to 3% from the eight shell results. Only our five shell results are quoted in the Table.

Corrections to the forces (11) have been included for all five shells. The results for the forces in the displaced positions showed that these corrections are significant for first and second neighbours and negligible for the fourth and fifth, in agreement with conclusion of Flocken and Hardy (1969). As a representative example, for Na in Rb we quote in Table I the forces on the atoms in their nondisplaced and the displaced positions as well as the displacements for the first five shells.

Table I

Forces and displacements of the first five shells for Na in Rb. a is the cubic unit cell lattice parameter

Neighbour	Component	Force/a (dyn/cm) displaced	Force/a (dyn/cm) nondisplaced	Displacement (in units of a)
111	x=y=z	-89.34	-129.69	-0.03099
200	x (y=z=0)	-29.39	- 17.93	0.01532
220	x=y (z=0)	5.17	5.96	-0.00810
311	x	- 4.26	- 4.56	0.00142
	y=z	- 1.52	- 1.52	-0.00121
222	x=y=z	- 2.45	- 2.76	-0.01637

Vacancy and impurity resistivities for all combinations of alkali metals were calculated for both relaxed and nonrelaxed lattices. The results of the calculations, together with the existing experimental results are given in Table II. The overall agreement with experiment is reasonably good, perhaps it is even slightly better than that obtained by Dickey et al. (1967), as the result for Cs is considerably closer to experiment. The inclusion of relaxation does not improve the overall agreement. However, apart from the possible experimental error, one should not anticipate great accuracy from the one parameter Ashcroft pseudopotential applied on two very different properties of a material. The core radii due to Price et al. (1970) were fitted to the phonon neutron scattering data and we have applied them to the electrical resistivity. As the weighting factors for calculation of resistivity and interionic forces are different, there is some intrinsic uncertainty in applying the same one parameter pseudopotential to both properties.

6. Conclusion

The main result of our paper is the change of the residual resistivity due to lattice relaxation. We see that the correction is around 5-30%, thus confirming the estimate of Ziman (1964) who predicted a correction of the order of 10%. It is also interesting to note that the lattice relaxation, while decreasing the residual resistivity of vacancies (in agreement with Benedeck and Baratoff 1971), increases the residual resistivity of substitutional impurities.

Table II

Experimental and theoretical residual resistivities for dilute alkali alloys. Experimental results were collected by Dickey et al. (1967). Theoretical are given for nonrelaxed and relaxed lattice.

Solvent	Solute	Residual Resistivity ($\mu\Omega$ cm/at %) exp.	nonrelaxed	relaxed
Li	vacancy	-	1.005	0.759
	Na	-	0.426	0.458
	K	-	3.084	3.288
	Rb	-	4.193	4.483
	Cs	-	5.529	5.958
Na	Li	-	0.305	0.341
	vacancy	-	1.207	0.888
	K	-	1.112	1.184
	Rb	-	1.903	2.021
	Cs	-	3.108	3.297
K	Li	-	2.288	2.914
	Na	0.56	1.037	1.272
	vacancy	-	1.353	0.975
	Rb	0.11	0.117	0.136
	Cs	1.1	0.595	0.689

Table II - continued

Solvent	Solute	Residual Resistivity (μΩ cm/at %) exp.	nonrelaxed	relaxed
Rb	Li	-	3.159	4.145
	Na	-	1.718	2.166
	K	0.04,0.13	0.112	0.134
	vacancy	-	1.434	1.050
	Cs	-	0.180	0.212
Cs	Li	-	4.470	6.107
	Na	-	2.810	3.672
	K	-	0.553	0.682
	Rb	0.28	0.175	0.213
	vacancy	-	1.559	1.182

APPENDIX C

ON THE DISPLACED LATTICE CHARGE AND RESIDUAL RESISTIVITY

(Popović and Carbotte 1974b)

Abstract

We have used the method of lattice statics to perform microscopic calculations of the displaced lattice charge far away from an impurity in an alkali metal. The displaced charge is then used to determine with the aid of the continuum approximation the change in solid structure factor and from it to estimate the correction to the residual resistivity due to strain. Our approximate results for this correction are compared with exact lattice static results and it is found that the continuum approximation very often seriously underestimates the effect of strain.

1. Introduction

When an impurity is introduced into an otherwise perfect lattice the neighbouring atoms will experience a change in the forces on them and they will come to new equilibrium positions. This atomic readjustment is an interesting problem and can have important effects. The necessity to correct the residual resistivity for lattice relaxation has been recognized in the past and approximate schemes have been developed to account for it. One approach (Blatt 1957) is to characterize the electron-impurity scattering by a set of phase shift and to modify the Friedel sum rule on these phase shift to include in it a correction for the amount of displaced lattice charge around the impurity. The size of the correction is to be estimated from the measured macroscopic volume change. Another approach (Harrison 1966) is to use a pseudopotential for the electron-impurity scattering and to calculate in the continuum approximation the change in solid structure factor due to the impurity. The continuum structure factor is again to be determined from experiments on the volume change. Both methods deal only with large distance information and employ experimental data.

On the other hand the method of lattice statics (Kanzaki 1957, Flocken and Hardy 1969) can be used to calculate the atomic displacements about an impurity at short as well as large distances on a discrete lattice. This information can then be used to include in detail the effect of strain on residual resistivity (Popović, Carbotte, and Piercy 1973).

Such calculations are, however, complex and at present available only for a limited number of systems. Thus, they are not always that useful in interpreting and correlating experimental data and the simpler although approximate methods previously described are still being used. It is, therefore, of some importance to assess the accuracy of such approximate schemes. This is the aim of this paper and we now describe how we plan to do so.

Lattice statics calculations of the atomic displacements match up asymptotically to the results of continuum theory. Thus the displaced lattice charge at large distance from an impurity can be obtained with no reference to experiment and, in conjunction with a continuum approximation, used to obtain an estimate of the effect of strain on residual resistivity. It is then completely consistent to compare this estimate with the results of exact lattice statics computations in which the short range atomic displacements are accurately included. In this way it is possible to make a systematic and internally consistent study of the validity of the continuum approximation in resistivity calculations.

In Sect. 2 we sketch very briefly some of the main results of lattice statics and make connection with the total displaced lattice charge (Z^*). Numerical results for Z^* are tabulated and discussed. Section 3 is concerned with the effect of lattice relaxation on the residual resistivity (ρ_I). In Sect. 4 we calculate from Z^* the change in solid structure factor within the continuum approximation. We then use this structure factor to estimate the fractional change $(\Delta\rho_I/\rho_I)$ in ρ_I which we compare with exact results. A short discussion can be found in Sect. 5.

2. Lattice Statics and the Displaced Lattice Charge

Kus, Carbotte, and Bergersen (1973) and others have discussed the relationship between the displaced lattice charge due to a defect and the displaced volume. The displaced charge at large distances (Z^*) is obtained from

$$[1] \qquad Z^* = -\frac{\Delta\Omega}{\Omega_0} = -i \lim_{q\to 0} \int \frac{d\Omega_q}{4\pi} \underline{q}\cdot\underline{u}(\underline{q})$$

where $\Delta\Omega$ is the displaced volume and Ω_0 is the volume of a primitive cell. The integration over the angles of $\underline{q}$ ($d\Omega_q$) is to be performed and then the limit $q\to 0$ taken. In [1] $\underline{u}(\underline{q})$ stands for the Fourier transform of the real space atomic displacements $\underline{u}_{\underline{\ell}}$. That is

$$[2] \qquad \underline{u}(\underline{q}) = \sum_{\underline{\ell}} \underline{u}_{\underline{\ell}} e^{-i\underline{q}\cdot\underline{\ell}}$$

where $\underline{\ell}$ represent the perfect lattice equilibrium positions.

To calculate Z^* from [1] we need only to know the real space displacements $\underline{u}_{\underline{\ell}}$. They can be calculated from microscopic theory by the method of lattice statics which was developed by Kanzaki (1957), Flocken and Hardy (1969) and others. In this formalism the atomic displacements in $\underline{q}$-space $\underline{u}(\underline{q})$ are related to the array of forces due to the defect by

$$[3] \qquad \underline{u}(\underline{q}) = \underline{\underline{D}}(\underline{q})^{-1} \cdot \underline{F}(\underline{q})$$

with $\underline{\underline{D}}(\underline{q})$ the dynamical matrix for the perfect crystal and $\underline{F}(\underline{q})$ the Fourier transform of the real space forces $\underline{F}_{\underline{\ell}}$. Here $\underline{F}_{\underline{\ell}}$ is the force felt by the $\underline{\ell}$'th host atom. It can be computed from a knowledge of the host impurity potential. It should be remembered, however, that the $\underline{F}_{\underline{\ell}}$'s are to be evaluated at the new equilibrium positions so that the problem must be solved self-consistently (Popović, Carbotte, and Piercy 1973).

The driving potential due to a substitutional impurity is given by

$$[4] \qquad V_I(r) = Z_H(Z_I - Z_H)e^2/r - 2\frac{e^2}{\pi}\int_0^\infty G_I(q)\,\frac{\sin(qr)}{qr}\,dq$$

with

$$[5] \qquad G_I(q) = \left(\frac{4\pi e^2}{\Omega_0 q^2}\right)^{-2}\frac{W_H(q)\,\Delta W(q)}{1-f(q)}\left(1 - \frac{1}{\varepsilon(q)}\right)$$

In eq. [4] Z_H and Z_I are respectively the charge on the host and impurity ion. The electron charge is denoted by e and Ω is a position vector. In [5] W_H denotes the host while $W \equiv W_I - W_H$ denotes the difference between impurity and host pseudopotential. We will assume an Ashcroft empty core model which is then completely specified by giving the core radius (R_c):

$$W_{H(I)}(q) = -\frac{4\pi e^2}{q^2\Omega_0} Z_{H(I)}\,\frac{\cos(qR_c)}{\varepsilon(q)}$$

Values for R_c for the alkalis are entered in Table 1. The dielectric function $\varepsilon(q)$ which describes the screening by the conduction electrons is given by

Table 1

	Li	Na	K	Rb	Cs
R_c	1.40	1.69	2.226	2.40	2.62

The Ashcroft core radius (R_c) for the alkalis. R_c is in atomic units, i.e., in units of the Bohr radius a_0.

[6] $$\epsilon(q) = 1 + (1-f(q))Q(q)$$

where the factor f(q) takes into account correlation and exchange. It is taken from the work of Singwi et al. (1970). The only remaining quantity is the factor Q(q) in [6] which is the Lindhard polarization part given by

$$Q(q) = \frac{4\pi e^2}{q^2 \Omega_0} \left(\frac{2}{3} E_F\right)^{-1} \left\{\frac{1}{2} + \frac{4k_F^2 - q^2}{8k_F q} \ln\left|\frac{2k_F+q}{2k_F-q}\right|\right\}$$

where k_F is the Fermi momentum and E_F the Fermi energy. The theory is now completed and there remains only to present results.

In Table 2 we present results for Z* for vacancies as well as all possible choices for an alkali impurity in the alkalis.

We note that all the entries below the diagonal are positive while all those above are negative. This can be understood with reference to Table 1 where we give the R_c values for the alkalis. In a rough sort of way R_c can be considered to be the atomic core radius. Thus a small impurity or a vacancy leads to relaxation of the atoms inwards (at large distances) while an impurity that is large relative to a host atom gives an outward displacement, i.e., a negative Z*.

Having computed the Z*'s we would like to explore whether or not they bear any relationship to the effect of strain on the residual resistivity.

Table 2

Impurity / Host	Vacancy	Li	Na	K	Rb	Cs
Li	+.191	-	-.278	-.750	-.896	-1.077
	(-.245)	-	(.075)	(.066)	(.069)	(.078)
Na	+.224	+.248	-	-.413	-.540	-.696
	(-.265)	(.117)	-	(.065)	(.062)	(.061)
K	+.300	+.580	+.361	-	-.109	-.242
	(-.279)	(.274)	(.226)	-	(.164)	(.155)
Rb	+.311	+.663	+.453	+.105	-	-.128
	(-.268)	(.312)	(.261)	(.201)	-	(.177)
Cs	+.305	+.767	+.662	+.224	+.123	-
	(-.241)	(.366)	(.307)	(.234)	(.219)	-

The value of Z^* the displaced lattice charge for various alkali impurities in alkali hosts. Results for vacancies are also included. In the brackets we have recorded the fractional change $\Delta\rho_I/\rho_I$ in the residual resistivity due to lattice relaxation.

3. Residual Resistivity

To calculate the effect of lattice relaxation on the residual resistivity one first needs the change in solid structure factor due to the defect. It is

$$[7] \qquad \Delta S(\underline{q}) = - i\underline{q}\cdot\sum_{\underline{\ell}} \underline{u}_{\underline{\ell}} e^{-i\underline{q}\cdot\underline{\ell}} = - i\underline{q}\cdot\underline{u}(\underline{q})$$

where $\underline{u}(\underline{q})$ can be obtained from a lattice statics calculation. The residual resistivity ρ_I is given by (Popović, Carbotte, and Piercy 1973)

$$[8] \qquad \rho_I = \frac{3m^{*2}\Omega_0 n_I}{16\hbar^3 e^2 k_F^2} \int_{|\zeta|<2} |N\langle \underline{k}_F+\underline{q}|V_{scatt}|\underline{k}_F\rangle|^2 \, \zeta \, \frac{d^3\underline{\zeta}}{\varepsilon(q)^2}$$

with $\zeta = q/k_F$ and

$$[9] \qquad \langle \underline{k}'|V_{scatt}|\underline{k}\rangle = \frac{1}{N}\,[\{\Delta S(\underline{q})-1\}W_H(q) + W_I(q)] \quad .$$

In [8] m* is an electron effective mass, Ω_0 the volume per ion, n_I the number of impurities, $\hbar$ Planck's constant over 2π and e the charge on the electron. The Fermi momentum is k_F and the integration over momentum transfer $\underline{q}$ extends over a sphere of radius $2k_F$.

From eqs. [7], [8], and [9] a value for the residual resistivity can be obtained which includes the effect of strain within the framework of lattice statics. Results have been reported previously by Popović, Carbotte, and Piercy (1973).

Their results are entered in Table 2 and are to be compared with our results for Z*. What appears as a bracketed entry is the fractional change in residual resistivity due to strain. We first note that there appears to be no relationship as to absolute value between Z* and the fractional change in resistivity $\Delta\rho_I/\rho_I$. Second, the sign of these two quantities is not correlated. Thus, it is not possible to state in general that an inward displacement of the crystal at large distances will always lead to a decrease or increase in the resistivity. Both outcomes are possible.

If we look only at vacancies we see a closer, although not exact, correspondence between Z* and $\Delta\rho_I/\rho_I$. All the displacements are inward (i.e., positive Z*) and in all cases the resistivity is decreased by lattice relaxation. The volume changes vary in magnitude from 19 to 31% while the changes in resistivity (ρ_I) vary somewhat less from 22 to 27%. We note that strain has very nearly the same effect on ρ_I for a vacancy in Li as for one in Cs. The displaced charge is, however, quite different. In one case it is 19%, while in the other it is 31%. Still for vacancies Z* is a reasonable measure of the fractional change in ρ_I.

Actually we should not be comparing Z* directly with the fractional change in ρ_I ($\Delta\rho_I/\rho_I$) due to strain. Instead (following Harrison) we should use our results for Z* to calculate the change in structure factor in the continuum approximation and then use this approximate structure factor to get an estimate of $\Delta\rho_I$. We can then compare the estimate with our exact results. This is done next.

4. Continuum Approximation

Harrison (1966) suggests replacing the atomic displacements $\underline{u}_{\underline{\ell}}$ in [7] by their asymptotic form in an isotropic crystal, i.e., by

$$[10] \qquad \underline{u}_{\underline{\ell}} = \frac{A}{|\underline{\ell}|^3}\,\underline{\ell}$$

with the displacement taken to be radial. In [10] we take A to be equal to $-Z^*/4\pi$ where Z^* was calculated in Sect. 2. If we substitute [10] into [7] we get an approximation for the change in structure factor which we denote by $\Delta S^H(\underline{q})$ and which is given by

$$[11] \qquad \Delta S^H(\underline{q}) = (-Z^*/4\pi) \sum_{\underline{\ell}} \left[\frac{\cos(q|\underline{\ell}|)}{q|\underline{\ell}|} - \frac{\sin(q|\underline{\ell}|)}{(q|\underline{\ell}|)^2}\right] \frac{q}{|\underline{\ell}|^2} \cdot$$

Equation [11] is easily calculated from a knowledge of Z^* and the symmetry of the perfect lattice.

Table 3 refers to the case of vacancies in the alkalis. In the first column we have entered the value of the resistivity that is obtained when lattice relaxation is ignored. In column two we enter the change in residual resistivity $\Delta\rho_I$ obtained from a full lattice statics calculation using the structure factor [7]. In column three we have the results for $\Delta\rho_I$ using the approximate structure factor [11]. We see that the continuum approximation consistently underestimates the effect of strain on ρ_I by a factor of 2 to 4. This is a large

Table 3

ρ_I ($\mu\Omega$-cm/%) without relaxation	$\Delta\rho_I$ ($\mu\Omega$-cm/%) due to relaxation		Vacancy in
	ΔS	ΔS^H	
1.005	-.246	-.079	Li
1.207	-.319	-.108	Na
1.353	-.378	-.180	K
1.434	-.384	-.197	Rb
1.559	-.376	-.205	Cs

Resistivity due to vacancies in the alkalis. In column 1 we have ρ_I without strain in $\mu\Omega$-cm/%. In column 2 we have the change in ρ_I calculated from lattice statics which is to be compared with column 3 where Harrison's continuum approximation has been used to get $\Delta\rho_I$.

amount so that continuum approximation is obviously not applicable in this case.

To explore the situation further we consider several different impurities in the specific case of K. We will characterize the various impurities by an Ashcroft form with given Z_I and R_c and let both these parameters vary over some representative range of realistic values. Specifically we will explore the case of Z_I = 1, 2 in potassium and allow R_c to vary between 1 and 2.6 atomic units. Our results are summarized in Fig. 1 where we plot $\Delta\rho_I/\rho_I$ as a function of R_c. For the case of Z_I = 1, a dashed line has been used to join the 9 points at which calculations were performed. For Z_I = 2, a solid curve is employed. Dots indicate the results of the complete theory while crosses give the results of a continuum approximation. We first note that for Z_I = 1 strain increases the resistivity and that the continuum approximation consistently underestimates by a large amount $\Delta\rho_I/\rho_I$ over the entire range of R_c considered. For Z_I = 2 the situation looks more complex because $\Delta\rho_I/\rho_I$ goes through zero and changes sign going from positive (an increase in ρ_I) to negative (a decrease in ρ_I) as R_c ranges from 1 to 2.6 atomic units. Still, except for the points at R_c = 2.6, $\Delta\rho_I/\rho_I$ is underestimated in absolute value by making use of the continuum approximation. At the discrete points where we have made calculations it does give the right sign. Still it is in general a poor approximation.

Before leaving this section it may be of interest to see how the structure factor $\Delta S(q)$ given by eq. [7] differs from its value $\Delta S^H(q)$ in the continuum approximation given by

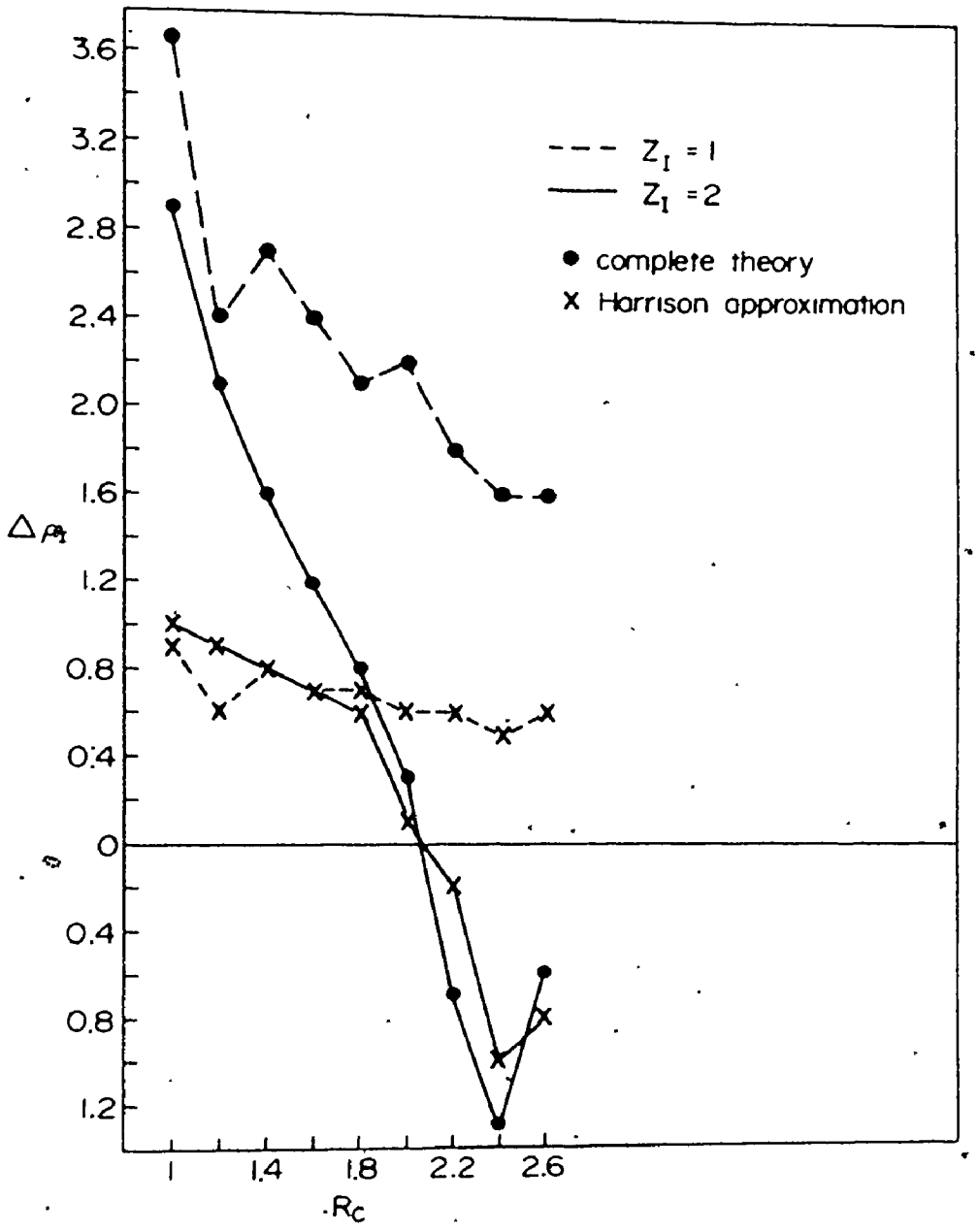

Fig. 1: Change in the residual resistivity $\Delta\rho_I$ due to lattice relaxation as a function of the impurity core radius R_c in atomic units. The dashed line indicates the case of the impurity charge Z_I equal to 1 while the solid curve is for $Z_I = 2$. The dots indicate the results of the complete lattice statics calculation while the crosses result from the use of the continuum approximation for the

eq. [11]. Actually it is not very convenient to compare these two quantities directly since $\Delta S(\underline{q})$ depends on the angles of $\underline{q}$ as well as on its absolute value. To get around this difficulty we introduce the angular average of $\Delta S(\underline{q})$ which we denote by $\Delta S^M(q)$. It depends only on the absolute value of $\underline{q}$ and is given by

$$[12] \qquad \Delta S^M(q) = \int \frac{d\Omega_{\underline{q}}}{4\pi} \Delta S(\underline{q}) \quad .$$

The mean structure factor $\Delta S^M(q)$ is a useful quantity only in as much as it gives very nearly the same fractional change in resistivity $\Delta\rho_I/\rho_I$ as does the complete $\Delta S(\underline{q})$. This is certainly the case for Rb in K which we will now discuss. With the exact $\Delta S(\underline{q})$, eq. [7], we get a value of $\Delta\rho_I = .019$ while with [12] we get $\Delta\rho_I = .018$ which is close enough to .019 since the continuum result is only $\Delta\rho_I = .006$. Having made sure that the angular average in [12] is not of any great numerical significance we compare in Fig. 2a $\Delta S^M(q)$ with $\Delta S^H(q)$. The only range of interest for q is from 0 to $2k_F$ since the integral in the expression [8] for ρ_I cuts off at $2k_F$. We note that in the limit $q \to 0$ the two structure factors match up but that they rapidly start diverging as q increases towards $2k_F$. It is also important to note that while they both start off to be negative (the displaced volume is outwards) they go through zero and then become positive. It is this positive region that wins out in the integral for ρ_I since strain increases the resistivity for Rb in K. That the region near $2k_F$ is very important can be seen directly from expression [8]. A q^3 weighting

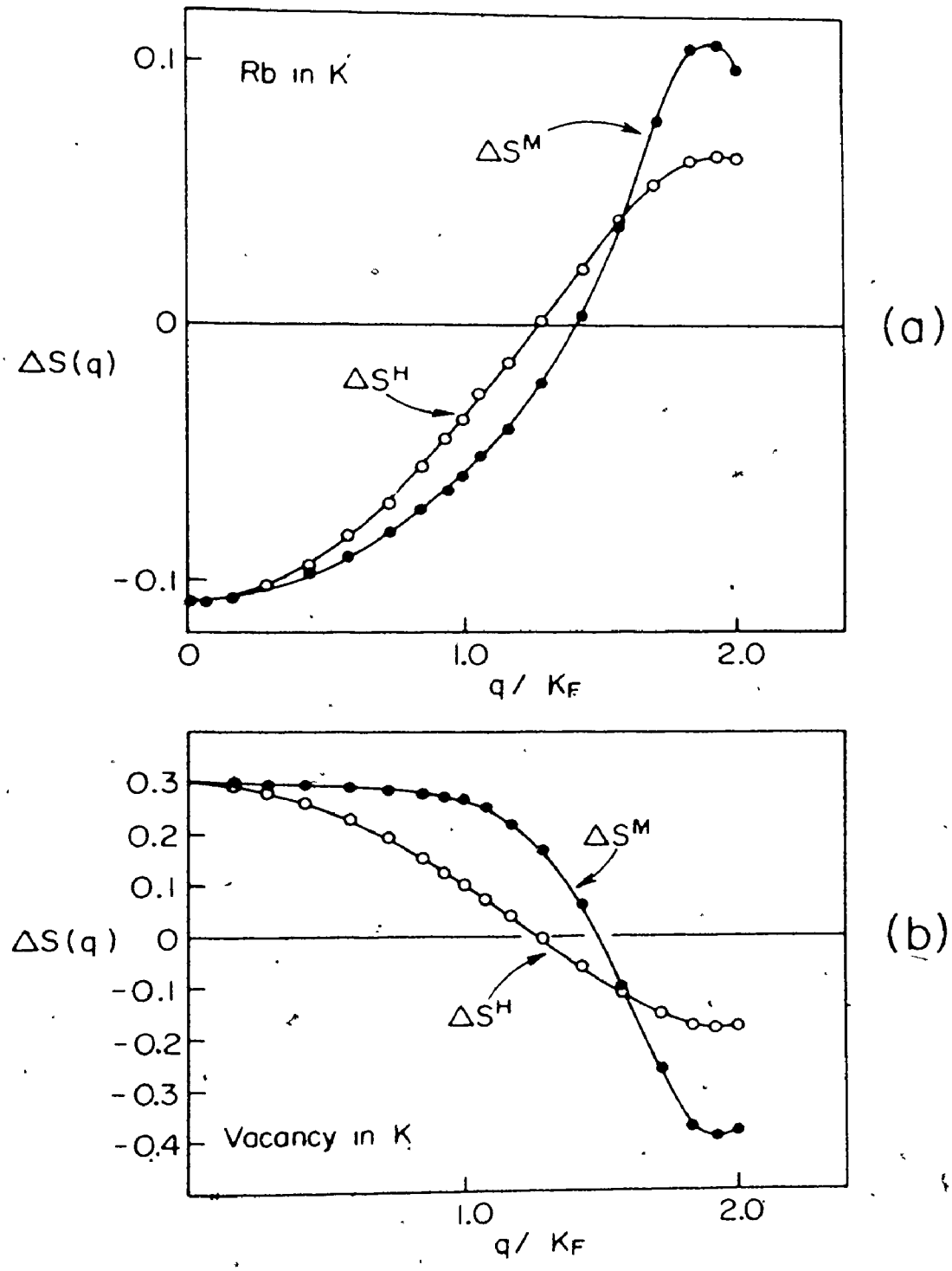

Fig. 2: The change in the structure factor $\Delta S^M(q)$ versus q compared with its value in the continuum approximation $\Delta S^H(q)$: a) for Rb in K, b) a vacancy in K.

is evident which weights heavily the region near $2k_F$. From an examination of Fig. 2a, keeping in mind that it is not the $q \to 0$ region that is important, we see no simple correction or prescription that can be applied to $\Delta S^H(q)$ so as to make it look more like $\Delta S^M(q)$ and thus improve the continuum approximation. A full calculation is needed to get quantitatively reliable results. We have found, however, that it is always a reasonable approximation to use $\Delta S^M(q)$ in [8] rather than $\Delta S(q)$. This introduces an important simplification so that future calculations could use this approximation instead of the continuum approximation.

In Fig. 2b we show results for the case of a vacancy in K. The two structure factors again match up at $q \to 0$. They start positive (the displaced volume is inwards) and end up negative. In the region of importance $\Delta S^M(q)$ bears no simple relation to $\Delta S^H(q)$. To be complete, it should be noted that with $\Delta S(q)$ we get $\Delta\rho_I = -.378$ to be compared with $\Delta\rho_I = -.457$ when $\Delta S^M(q)$ is used and $\Delta\rho_I = -.180$ for the continuum approximation. The average structure factor is not as good an approximation in this case as it was for Rb in K. It is, however, still much better than the continuum approximation.

5. Conclusion

We have calculated the macroscopic displaced lattice charge (Z*) about various impurities in the alkalis. We have compared these values with the fractional change in the residual resistivity $\Delta\rho_I/\rho_I$ due to strain. We find no simple relationship between the two. We use our results for Z* to calculate $\Delta\rho_I/\rho_I$ making use of the continuum approximation for the solid structure factor. We find that the continuum approximation very often seriously underestimates $\Delta\rho_I/\rho_I$. It has been used widely in the past. To get quantitatively significant results, it is necessary to make complete lattice statics calculations although we believe that it is often sufficient to approximate the structure factor by its angular average. This greatly simplifies the computations.

APPENDIX D

SHORT DESCRIPTION OF COMPUTER PROGRAMS

The following are the main programs developed during this work.

1. Program for calculation of vacancy formation energy and volume in bcc and fcc crystals. Input data: crystal structure, lattice parameter, bulk modulus, ionic charge. Output: force constants, displacements of nearest neighbours around a vacancy, vacancy formation energy and volume and a number of intermediate results, including different terms contributing to the vacancy formation energy and volume.

2. Program for calculating heat of solution of hydrogen in fcc and hcp crystals using pseudopotential (linear response) theory. Lattice relaxations not included. Input data: crystal structure, lattice parameter, c/a ratio (if applicable), binding energy, ionic charge. Output: heat of solution and the values of different terms contributing to it.

3. Program for the calculation of nonlinear proton screening (a modified version of the program supplied by M. Stott, Department of Physics, Queen's University, Kingston, Ontario). Input data: density parameter of the electron gas r_s, proton charge Z_p, trial potential parameter b (Equation (5.33)), Output: phase shifts, potential and density fluctuations as a function of distance, Friedel sum.

4. Program for calculating displacements around vacancy in hexagonal metals. Input data: radial and tangential force constants. Output: forces in relaxed positions, displacements.

5. Program for calculating residual resistance of alkali impurities in alkali metals. Input data: lattice parameter of the host lattice, effective mass, parameters in the function for exchange and correlation corrections for the dielectric function (Appendix B, Equation (18)), Ashcroft empty core model potential radii for the host and impurity ions. Output: nearest neighbour displacements around the impurity, residual resistivities for nonrelaxed and relaxed lattices.

REFERENCES

Abarenkov I V and Heine V 1965 Phil. Mag. 12 529-37

Animalu A E O and Heine V 1965 Phil. Mag. 12 1249-69

Béal-Monod M T and Kohn W 1968 J. Phys. Chem. Solids 29 1877-87

Benedeck R and Baratoff A 1971 J. Phys. Chem. Solids 32 1015-24

Blatt F J 1957 Phys. Rev. 108 285-90

Blatt F J 1957 Phys. Rev. 108 1204-6

Boyer L L and Hardy J R 1971 Phys. Rev. B 4 1079-88

Bullough R and Tewary V K 1972 Interatomic Potentials and Simulation of Lattice Defects eds. P C Gehlen, T R Beeler Jr and R I Jaffee (New York and London: Plenum Press) 155-76

Carbotte J P 1967 Phys. Rev. 155 197-207

Chang R and Falicov L M 1971 J. Phys. Chem. Solids 32 465-73

Cohen M L and Heine V 1970 Sol. St. Phys. 24 eds. H Ehrenreich, F Seitz and D Turnbull (New York and London: Academic Press) 56

De Wames R E, Wolfram T and Lehman G W 1965 Phys. Rev. 138 A717-28

Dickey J M, Meyer A and Young W H 1967 Phys. Rev. 160 490-6

Du Charme A R and Weaver H T 1972 Phys. Rev. B 5 330-5

Eichenauer W 1968 Z. Metallkde. 59 613-6

Emley E F 1966 Principles of Magnesium Technology (Oxford: Pergamon Press)

Emrick R M and McArdel P B 1969 Phys. Rev. 188 1156-62

Feder R 1970 Phys. Rev. B 2 828-34

Feder R and Charbnau H P 1966 Phys. Rev. 149 464-71

Fetter A L and Walecka J D 1971 Quantum Theory of Many-Particle Systems (New York: McGraw-Hill) 69-70

Flinn P A and Maradudin A A 1962 Ann. Phys. 18 81-109

Flocken J W and Hardy J R 1969 Phys. Rev. 177 1054-62

Friedel J 1952 Phil. Mag. 43 153-89

Fukai Y 1969 Phys. Rev. 186 697-704

Fumi F G 1955 Phil. Mag. 46 1007-20

Green M P and Kohn W 1965 Phys. Rev. 137 A513-22

Handbook of Chemistry and Physics 1970 ed. R C Weast (Cleveland, Ohio: The Chemical Rubber Co.)

Hardy J R 1968 J. Phys. Chem. Solids 29 2009-14

Harrison W A 1966 Pseudopotentials in the Theory of Metals (New York: Benjamin Press) 204-6

Harrison W A 1970 Solid State Theory (New York: McGraw-Hill) 200-12

Hedin L and Lundqvist B I 1971 J. Phys. C: Solid St. Phys. 4 2064-83

Heine V and Abarenkov I V 1964 Phil. Mag. 9 451-65

Ho P S 1971 Phys. Rev. B 3 4035-43

Ho P S 1972 Interatomic Potentials and Simulation of Lattice Defects eds. P C Gehlen, T R Beeler Jr and R I Jaffee (New York and London: Plenum Press) 321-38

Hohenberg P and Kohn W 1964 Phys. Rev. 136 B864-71

Hultsch R A and Barnes R G 1962 Phys. Rev. 125 1832-42

Kamm G N and Alers G A 1964 J. Appl. Phys. 35 327-30

Kanzaki H 1957 J. Phys. Chem. Solids 2 24-36

Kenny P N, Trott A J and Heald P T 1973 J. Phys. F: Metal Phys. 3 513-22

Koeneman J and Metcalfe A G 1959 Trans. ASM 51 1072-82

Kohn W and Sham L J 1965 Phys. Rev. 140 A1133-38

Kolachev B A 1968 Hydrogen Embrittlement of Nonferrous Metals (Jerusalem: Israel Program for Scientific Translations)

Kus F, Carbotte J P and Bergersen B 1973 J. Phys. F: Metal Phys. 3 1061-70

Lang N D and Kohn W 1971 Phys. Rev. B 3 1215-23

Langer J S and Vosko S H 1960 J. Phys. Chem. Solids 12 196-203

Lidiard A B 1972 private communication

MacDonald D K C 1953 J. Chem. Phys. 21 177-8

March N H and Murray A M 1960 Proc. Roy. Soc. A256 400-15

March N H and Rousseau J S 1971 Crystal Lattice Defects 2 1-46

McKee B T A, Triftshauser W and Stewart A T 1972 Phys. Rev. Lett. 28 358-60

McLellan R B 1973 J. Phys. Chem. Solids 34 1137-41

Meyer A, Young W H and Hayes T H 1971 Phil. Mag. 23 977-86

Mueller W M, Blackledge J P and Libowitz G G 1968 Metal Hydrides (New York: Academic Press)

Mukherjee K 1965 Phil. Mag. 12 915-8

Pines D and Nozieres P 1966 The Theory of Quantum Liquids Vol. 1 (New York: Benjamin Press) 330

Popović Z D and Carbotte J P 1974a J. Phys. F: Metal Phys. (accepted for publication); Appendix A of the thesis

Popović Z D and Carbotte J P 1974b Can. J. Phys. (submitted for publication); Appendix C of the thesis

Popović Z, Carbotte J P and Piercy G R 1973 J. Phys. F: Metal Phys. 3 1008-14; Appendix B of the thesis

Popović Z D, Carbotte J P and Piercy G R 1974 J. Phys. F: Metal Phys. 4 351-60

Price D L, Singwi D S and Tosi M P 1970 Phys. Rev. B 2 2983-99

Pynn R and Squires G L 1972 Proc. Roy. Soc. (London) 326 347-60

Shaw R W 1968 Phys. Rev. 174 769-81

Shaw R W 1969 J. Phys. C: Solid St. Phys. 2 2335-49

Shaw R W and Pynn R 1969 J. Phys. C: Solid St. Phys. 2 2071-88

Shyu W M, Brust D and Fumi F G 1967 J. Phys. Chem. Solids 28 717-24

Shyu W M and Gaspari G D 1968 Phys. Rev. 170 687-93

Simmons R O and Balluffi R W 1960 Phys. Rev. 117 52-61

Singwi K S, Sjölander A, Tosi M P and Land R H 1970 Phys. Rev. B 1 1044-53

Sjölander A and Stott M J 1972 Phys. Rev. B 5 2109-18

Smialowski M 1962 Hydrogen in Steel (Oxford: Pergamon Press)

Tewary V K 1973 J. Phys. F: Metal Phys. 3 704-8

Tosi M P 1964 Sol. St. Phys. 16 107-13

Wenzl H 1970 Vacancies and Interstitials in Metals eds. A Seeger, D Schumacher, W Schillings and J Diehl (Amsterdam: North-Holland) 379

Ziman J M 1964 Advan. Phys. 13 89-138

Ziman J M 1972 Principles of the Theory of Solids (Cambridge University Press) 23-6